KU LEUVEN

FACULTY OF BIOSCIENCE ENGINEERING

Quantifying and understanding the relation between woody cover dynamics and temporal stability of Australian savannas

Kwantificeren en inzicht verwerven in de relatie tussen houtachtige begroeiingsdynamieken en temporele stabiliteit van Australische savannes

Promotors:
Prof. dr. ir. Ben Somers
Department of Earth and Environmental Sciences
Division of Forest, Nature and Landscape

Dr. ir. Wanda De Keersmaecker
Department of Biosystems
Division of Crop Biotechnics

Dissertation presented in
Fulfillment of the
requirements for the degree of
Master of Science in Agro- and
Ecosystems Engineering

Nora Oosters

June 2017

KU LEUVEN

FACULTY OF BIOSCIENCE ENGINEERING

Quantifying and understanding the relation between woody cover dynamics and temporal stability of Australian savannas

Kwantificeren en inzicht verwerven in de relatie tussen houtachtige begroeiingsdynamieken en temporele stabiliteit van Australische savannes

Promotors:
Prof. dr. ir. Ben Somers
Department of Earth and Environmental Sciences
Division of Forest, Nature and Landscape

Dr. ir. Wanda De Keersmaecker
Department of Biosystems
Division of Crop Biotechnics

Dissertation presented in
Fulfillment of the
requirements for the degree of
Master of Science in Agro- and
Ecosystems Engineering

Nora Oosters

June 2017

AKNOWLEDGEMENTS

I feel privileged that I received the opportunity to write a thesis on this interesting topic that focuses on the future prospects and challenges of the Australian savannas, and for this I am grateful to my promotor Professor Ben Somers and my co-promotor and daily supervisor Wanda De Keersmaecker.

Research and fieldwork took me to Australia, meeting wonderful, highly professional people with passion for science and research. I thank Professor Bradley Evans from the University of Sydney for taking me under his wings and introducing me into his team (Matthew Northwood, Lindsay Hutley and Kip Crossing), for his guidance, his enthusiasm, his commitment and, for taking the initiative to enrol me to the Indigenous Tour through Northern Territory. I thank Ian Marang for his invaluable assistance, his patience, and being my professional buddy out there in Litchfield National Park. I moreover want to thank Linda Luck for her great spirit and for helping us out with the vegetation survey on field.

Continuing my work in Leuven, I received great support from my promotor Professor Ben Somers. I thank him for this and for his positive and constructive attitude, as well as his good advice and decisions that pushed me towards achieving my goal. I thank Wanda De Keersmaecker for guiding me through this field of specialty that was new to me, for passing on some of her skills and techniques, for offering support and options when I got stuck, for her patience, and for correcting all my writings with so much detail and love for language.

Furthermore, I thank my parents and friends for their support the whole year through. I want to thank my mom in particular, for going meticulously through some of my writings and taking on the challenge every time to improve phrases to our mutual satisfaction.

SUMMARY

The Australian tropical savannas are a unique and dynamic ecosystem, and thrive on the tight coexistence between the discontinuous woody overstorey and the continuous grass understorey. While the grass layer has control over the dynamics of this ecosystem, the long-living woody cover layer determines mainly the long-term trends in vegetation productivity. In order to get some insight in the future prospects of this ecosystem, given the ongoing climate change, understanding and quantifying the woody cover dynamics and how this changing vegetation responds to short-term climate anomalies is of utmost importance. In this perspective, this study focuses on Litchfield National Park, situated in northern Australia, and aims to (i) quantify the woody cover dynamics from 2002 to 2016 using satellite observations and (ii) define the impact of these woody cover dynamics on the ecosystem's stability in space and time. Woody cover dynamics were assessed using the Dry Season Index (DSI), developed by Brandt et al. (2016), and confirmed that woody thickening is taking place in Litchfield National Park with an overall slight increase in woody cover up to 2.29% of the overall mean woody cover. This growth can mainly be attributed to the variability in climate, a changing fire regime and a rising CO_2 level. The short-term stability of the ecosystem was in this study characterized by the vegetation resilience and variance to Normalized Difference Vegetation Index (NDVI) anomalies. The impact of this woody cover increase on the resilience pointed towards a faster recovering and thus more resilient ecosystem. An increase in woody cover resulted moreover in an increase of the variance at the spatial level but was countered with a decreasing variance at the temporal level, giving no closure yet on this subject. As stability may be driven by other variables besides the woody cover (DSI), impacts of both fire frequency and bare soil coverage on the stability were analysed as well. Results of fire frequency at the spatial level indicated a lower resilience and a higher variance, corresponding to a higher susceptibility of the ecosystem, but could not be confirmed at the temporal level. Increases in bare soil coverage lastly had again a positive impact on the ecosystem as it fastened the recovery speed, making it more resilient, and decreased the variance, making it less susceptible to climate anomalies. It has however to be taken into account that woody cover, fire frequency and bare soil coverage are correlated, causing biased effects of each factor separately, and thus results from this study require to be addressed with caution.

ABRREVIATIONS AND SYMBOLS

BRDF: Bidirectional Reflectance Distribution Function

CRU: Climate Research Unit

DSI: Dry Season Index

ITCZ: Inter-Tropical Convergence Zone

MAP: Mean Annual Precipitation

MIR: Mid-Infrared part of spectrum (1 µm to 4 µm)

MODIS: Moderate Resolution Imaging Spectroradiometer satellite

NDVI: Normalized Difference Vegetation Index

NIR: Near Infrared part of spectrum (700 nm to 1 µm)

PAR: Photosynthetically Active Radiation

RGB: Red, Green and Blue band of spectrum

RMSE: Root Mean Square Error

SPEI: Standardized Precipitation-Evapotranspiration Index

SRTM: Shuttle Radar Topography Mission

SWIR: Short Wave Infrared spectrum (1.25 µm to 2.6 µm)

TIR: Thermal Infrared part of spectrum (4 µm to 15 µm)

UV: Ultraviolet part of spectrum (10 nm to 400 nm)

VCF: Vegetation Continuous Fields

VI: Vegetation Indices

VIF: Variance Inflation Factor

VIS: Visible part of spectrum (400 nm to 700 nm)

WGS84: World Geodetic System 1984

λ: Reflectance of a certain band or range of spectrum

β: Estimated predictor variable

LIST OF TABLES

LIST OF FIGURES

CONTENT

1 INTRODUCTION

Ecosystem dynamics, the study of how ecosystems regulate themselves and change through time (Complexity Academy 2016), has become more and more a topic of global interest (Filatov et al. 2005; Keitt 2008; Hull et al. 2015). Ecosystems, as communities of fauna and flora in conjunction with their environment, are being steered through a network of biotic and abiotic interactions (Boundless 2016). Through negative and positive interaction loops, and with the aid of specific key drivers, these entities develop in certain directions. Disturbances however play a major role and are known as phenomena that ecosystems cannot counterbalance, they pull it outside of its normal operating parameters and can change the original direction entirely (Mori 2011; Complexity Academy 2016). With the ongoing climate change these disturbance events, also called climate extremes and anomalies, will occur more frequently and with higher intensity. The climate variability and the higher occurrence of these extremes such as heatwaves, droughts, floods, cyclones and wildfires reveals significant vulnerability and exposure of some ecosystems (IPCC 2014). To evaluate the stability of an ecosystem to such events, several indicators, focusing either on the magnitude, duration, frequency or change over space and time of the disturbance event, or the strength of the ecosystem, can be used to describe the ecological stability (Donohue et al. 2016). To describe the short-term stability of the Australian savanna ecosystem in this master thesis research the focus will be put on the resilience and variance of the ecosystem. In literature there is a difference made between ecological resilience and engineering resilience. The former is defined as the magnitude of disturbance that can be absorbed before the system changes its structure by adjusting the variables and processes that regulate its behaviour (Holling 1996). Engineering resilience expresses the rate at which an ecosystem recovers after the disturbance (van Rooijen et al. 2015; De Keersmaecker, Lhermitte, et al. 2015)[1]. Variance is the inverse of stability and is measured as the variability over space or time (Donohue et al. 2016).

The ecosystem dynamics of the Australian savannas, that are known to already experience one of the most seasonal climates of the world's savannas (Hutley & Beringer 2011), are significantly exposed to climate change. Rising temperature levels, more frequent cyclone events and increasing frequency and intensity of rainfall events cause serious impacts on this tropical ecosystem that is built on a tight relationship between the woody overstorey and the grass understorey (Laurance et al. 2011). While the grass layer controls the dynamics of this ecosystem, the long-term trends in vegetation productivity are mainly determined by the long-living woody upper layer (Brandt et al. 2016). Disturbance events that affect this relationship and thereby the tree-grass ratio can seriously disrupt the structure and functioning of this savanna ecosystem, and therefore also its resilience and variance. A lot of research

[1] In the remainder of this thesis research engineering resilience will be referred to as 'resilience'.

has yet been done on describing the phenology patterns of Australian savanna ecosystems (Bowman et al. 2001; O'Grady et al. 2000) as well as forecasting the directions the system will take. Is woody cover taking over or are fire events occurring more frequently and thus reducing the woody vegetation? Predictions are made about the future of the ecosystem which provides implicit information on the stability, but research on the direct influence of woody cover dynamics on the stability of the system are lacking. In this perspective, the aim of this master thesis research is to quantify the short-term stability of the Australian tropical savanna ecosystem and investigate which role woody cover dynamics have in this story.

The magnitude of projects like this whereby dynamics over time have to be monitored does not allow anymore to only rely on field measurements, but needs also tools that enable frequent follow-ups of vegetation dynamics. The technology of remote sensing, known as the science of identifying, observing and measuring objects from a distance, has since the 1950's (Cohen 2000) taken a bigger role in the surveillance of ecosystem dynamics. With the rapid evolution of imaging techniques and time series analysis, studying the evolution of biological entities using satellite observations has not only become easier, but it has also broadened the scope for more ambitious goals.

2 LITERATURE STUDY

2.1 Savanna ecosystems

According to the World Wildlife Fund (WWF) the terrestrial world can be subdivided into 14 biomes, which can be described as entities of fauna and flora that have common characteristics due to similar climatic conditions, and 8 biogeographic realms (Olson et al. 2001). Savannas, belonging to the tropical and subtropical grasslands, savannas and shrublands biome, cover around 33 million km² (or around 22% of the land surface on Earth) of the world and appear mainly on three of the seven continents: Africa, Australia and South-America (Hill et al. 2012). Globally they contribute to approximately 30% of all terrestrial ecosystem gross primary productivity (House & Hall 2001) and on Australian level they form an undescribed component of the Australian carbon cycle (O'Grady et al. 2000). According to Ahlström et al. (2015) semi-arid ecosystems have a predominant role globally in driving the net biome flux and might even become more important given the future impacts of climate change. Although covering several continents, there exist enormous variations between the different continents based on the exact composition of the ecosystem. According to Lehmann et al. (2011) the presence of the savanna ecosystem depends on four determinant factors, namely effective rainfall, rainfall seasonality, soil fertility and to a lesser extent, the topographic complexity of landscapes. Looking at the rainfall patterns, savannas in South-America are considered to be the wettest (up to 2500 mm mean annual precipitation (MAP)) and show more seasonally concentrated annual rainfalls than the savannas on the African and Australian continent. The MAP range of the African savanna is the most narrow one and variates between 250 mm and 1750 mm, and the MAP of the Australian savannas ranges between 150 mm and 2000 mm. Savanna ecosystems are generally known as highly seasonal ecosystems as there exist extreme fluctuations in rainfall patterns, resulting in the typical monsoonal climate with a dry and wet season. Due to the geographical distribution across the three continents, the timing of these seasons differs greatly. But even on a continent scale the dry-wet season pattern can differ as some countries in Africa, mainly on the eastern part of the continent, feature two rain seasons (Hill et al. 2012), i.e. a long and short rainy season.

Focusing to the fertility factor, again the subdivision can be made between less fertile soils in the South-American savannas (e.g. in Brazil and Venezuela) whereas the African and Australian soils enjoy a higher fertility (Lehmann et al. 2011). A last difference that can be noticed between the continents has to do with the fauna that habitats the ecosystem. With the elephant, buffalo, giraffe, zebra and a lot of antelopes walking around, the African savannas face an important disturbance event that the other continents are less acquainted with. These mega-herbivores have a tremendous impact on the vegetation and environment as the browsing and trampling processes of these species influences the

growth and coexistence between the woody plants and grass species (Asner et al. 2009; Lehmann et al. 2011).

2.2 The Australian tropical savanna ecosystem

Zooming in on Australia, the tropical savanna ecosystem covers almost one quarter of the country (Fox et al. 2001) and spreads from the Kimberley region in Western Australia over the northern half of the Northern Territory to the Gulf of Carpentaria in north Queensland (Hutley & Beringer 2011). According to Bowman & Prior (2005) the Australian savanna ecosystem behaves uniquely compared to the other savannas of the world. With a dominance of evergreen species the Australian savannas go against all expectations of a typical deciduous overstorey in seasonally dry tropics. This can be partly explained by the particular climate of the northern part of the continent, that, based on a wet-dry gradient, causes again a subdivision in two biogeographical regions with distinct phenology patterns. The northern more coastal areas of the savanna ecosystem have an intensely seasonal climate, influenced by the annual movement of the Inter-Tropical Convergence Zone (ITCZ) (Bowman & Prior 2005; Hutley & Beringer 2011). This ITCZ drives the Australian summer monsoon, inducing high inter-annual variabilities in rainfall seasonality and intensity, and causing high air temperatures (Bowman & Prior 2005). Hereby it creates a stark division between the rainy season and dry season and makes the savannas one of the most dynamic biomes (Ma et al. 2013). Moving to the south, the climate is steered by the El Niño/El Niña phenomenon, causing a less strict division between the rainy and dry season (Jacklyn et al. 2016), and in general a drier climate. Looking from a vegetation point of view, there is a transition visible from savannas in the north dominated by an overstorey of evergreen *Eucalyptus* and *Corymbia* species with an understorey dominated by C4 annual and perennial tussock grasses, towards a dominance of *Acacia* wood- and shrublands with hummock grasslands in the southern parts (Ma et al. 2013; Hutley & Beringer 2011).

2.3 The dynamics of trees and grasses

When observing the tree-grass relationship from different perspectives, it becomes clear that the coexistence of both plant types are key to the uniqueness of this ecosystem. From a biological perspective the Australian tropical savanna ecosystem can be described as a bioregion built up as a two-layer mixture of a discontinuous stratum of woody overstorey and a continuous layer of herbaceous understorey plants (Figure 2.1). The latter layer predominantly consists of annual and perennial grasses whereas the former layer ranges from substantial trees to shrubs and palms (Hill et al. 2012; Lehmann et al. 2014). As an ecosystem consisting primarily out of two contrasting lifeforms,

savannas can be seen as a point in a continuous spectrum with on the one side grasslands as extreme and on the other extreme forests (Accatino et al. 2010). Looking at the temporal variations in greenness of vegetation of the Australian tropical savanna ecosystem, grasses can be defined as the seasonal component whereas trees are the persistent component of the green signal. With the beginning of the dry season in April, grasses will dry out and become non-photosynthetic while the trees are predominantly evergreen and stay photosynthetically active. The grass layer, controlling the dynamics of the ecosystem, will at the beginning of the wet season in November sprout again and contribute to the green scenery (Guerschman et al. 2009; Zhou et al. 2016).

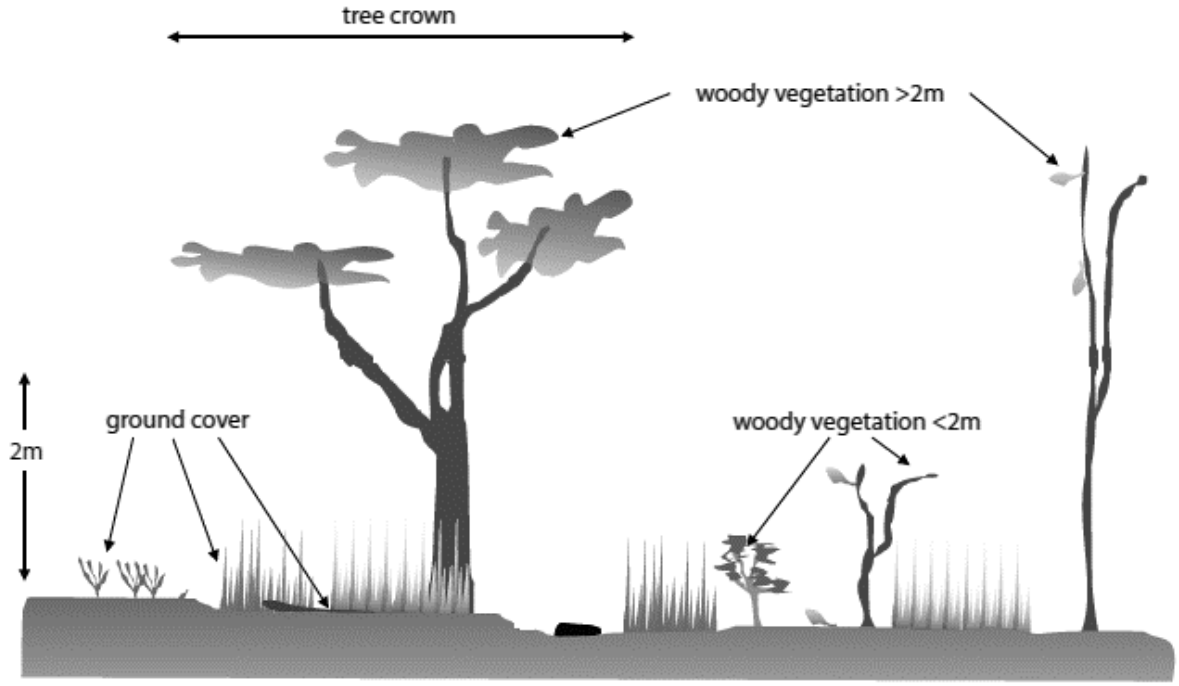

Figure 2.1: Schematic representation of Australian tropical savanna structure (adapted from Muir et al. 2011).

Trees and grasses interact with each other and the environment, and can either complement each other or compete with one another. Trees have lots of positive effects on grasses and herbal species but this has to be viewed in perspective, as the herbaceous diversity and production in savannas may be greater where there are a few trees than where there are no trees, but the trend is reversed at high tree densities. When evaluating the effects of trees on grasses, the effects of climate also have to be accounted for. From a temperature perspective, trees can improve harsh environmental conditions by providing shade and thus lower soil temperatures, but they can also prohibit grasses from growing due to too much shade which does not allow the grasses to photosynthesize. Similarly from a water management point of view, herbaceous production can either be enhanced under tree canopies in drier regions but can also be very harmful for the herbaceous understory where annual rainfall exceeds

a certain level, depending on the flora species and climate (Scholes & Archer 1997). A beneficial effect of trees on grasses is that they provide extra nutritional resources for grasses. These latter only have roots in the topsoil layer whereas trees have both roots in the topsoil layer as well as the subsoil layer and hereby can pump nutrients to higher soil layers. This niche separation of the roots allows a stable coexistence between grasses and trees (Accatino et al. 2010). Grasses can have on their side impacts especially on the recruitment of the overstorey. They can either directly compete for light, nutrients and water, or indirectly influence the overstorey as the amount of grasses defines the fuel load and thus fire frequency and intensity in savanna ecosystems. The impact of grass effects on trees depends heavily on the grass composition that is influenced by external factors like climate fluctuations, grazing and succession strategy. Changes in this composition can intensify or weaken the effects on trees (Scholes & Archer 1997).

2.4 Drivers of the tropical savanna ecosystem

The spatial patterns and composition of savannas, defined as tropical grasslands with scattered trees (Fox et al. 2001), are regulated by complex and dynamic interactions among climate, competition and disturbance events (Kanniah et al. 2011; Beringer et al. 2011; Scholes & Archer 1997). Climatic factors, including light, rainfall, temperature, CO_2 concentration and humidity, control the productivity of an ecosystem by regulating its water and nutrient availability, and are therefore indispensable drivers of the savannas (Beringer et al. 2011). The combination of all these climatic factors creates a unique environment where fauna and flora can grow, but also where competition can take place between organisms.

Every plant species is in need for light energy to grow and produce chemical energy via the photosynthesis process. As one of the basic ingredients, competition for light energy is ubiquitous between plant species, as between the herbaceous understorey and the evergreen overstorey layer in savannas. The herbaceous understorey, predominantly consisting of C4 grasses, cannot tolerate shading of sunlight to below a quarter of its open sky value, likely due to phylogenetic, environmental or physiological constraints. But at the hot conditions of the dry tropics, C4 grasses have a photosynthetic advantage which boosts a higher photosynthetic light-use efficiency than C3 types. Plants, utilizing this pathway, therefore started to dominate tropical grasslands and savannas. Besides competition for light energy, the understorey and overstorey vegetation also compete for nutrients and soil moisture in the upper soil layers (Osborne & Beerling 2006).

Disturbance events, as the third determinant component in the network of interactions, can create major impacts on the ecosystem by pulling it outside of its normal operating parameters. Savannas can suffer severely from cyclone events (Hutley et al. 2013), land clearing for agricultural purposes or fuel supply (Scholes & Archer 1997; Bristow et al. 2016), and grazing (Scholes & Archer 1997; Asner et al. 2009; Lehmann et al. 2011). Fire events are the greatest natural and anthropogenic environmental disturbances, that influence both the biophysical and biochemical processes from leaf to landscape scale. They have brand marked the structure, composition and distribution of the Australian savannas, as these ecosystems have coevolved with fire events (Beringer et al. 2015; Bristow et al. 2016). Looking from a historical-cultural point of view, indigenous people in Australia have used fire to hunt large games or to increase fertility and maintain habitat mosaics to increase the abundance of animal and vegetable resources (Bowman & Prior 2005; Scholes & Archer 1997; Fox et al. 2001). Besides fires started by humans, wildfires take often place during the dry season and can destroy hectares of land. Fires in the early dry season (late April to June) are typically of low intensity whereas fires at the end of the dry season (August to September) have a much higher intensity and destruction capacity due to a built-up of fuel load throughout the whole season and more extreme weather conditions (Beringer et al. 2015; Beringer et al. 2007; Lehmann et al. 2014). At last, climate change can also be seen as a disturbance event, evolving through time. One of the most influential widespread impacts of climate change is the increasing frequency and magnitude of climate extremes and anomalies. These extremes and anomalies can seriously disrupt the floristic composition and structural attributes of savannas (IPCC 2014).

2.5 Woody thickening of the Australian tropical savannas

Over the last 15 years, there has been a growing interest towards the question if woody biomass of the Australian tropical savannas is increasing (Chen et al. 2003; Beringer et al. 2007; Bowman et al. 2008; Lehmann et al. 2009). The vast majority of the studies reporting high rates of woody biomass increase over the past decades contrasts strongly with the studies of Lehman et al. (2009) and Murphy et al. (2014), who only remark a little net change in woody biomass. Judging from these observations it can be said that an increasing trend of woody cover has indeed taken place in the northern Australian savannas, but that the increase might not be as extensive as mentioned in a lot of studies. Factors that are being cited to cause this woody thickening phenomenon are overgrazing by domestic livestock and large-scale drivers like climate change (Murphy et al. 2014).

As recently indicated, a reduction of grass biomass due to overgrazing will reduce fire frequency and intensity and hereby favours the establishment of woody plants (Murphy et al. 2014). Due to climate

change, the temperature, rainfall and atmospheric CO_2 concentration, three basic ingredients for plant growth, have increased notably since the preindustrial time. Temperature and rainfall are two climatic factors that mark the length of the growing period, and thus influence the savanna productivity strongly. The CO_2 concentration of the atmosphere influences photosynthetic rates of the C3 and C4 plant species, their water-use efficiency and indirectly, the growing season length and reproduction of the whole system (Scheiter & Higgins 2009). As previously mentioned, an increase in the temperature levels favours the production of C4 plant species, that are omnipresent in the herbaceous understorey of the Australian savanna system. The augmenting frequency and intensity of rainfall events can have a positive impact on both C3 and C4 plant strategy groups. According to a study from Browning et al. (2008) in Arizona (USA), C4 grasses benefit from summer rains as only the upper soil layers get wetted at that moment due to a high evaporation rate at and a high interception rate from the tree leaves. C3 trees on the opposite profit more from winter rains because in this case water can also percolate to the deeper soil layers as there is a lower evaporation rate and almost no canopy cover and thus no interception from the tree. Shifts in these patterns for example towards more winter rains can boost the woody biomass. Similar phenomena were observed in the tropical savannas of Australia. Here however it were not the winter nor summer rains but the yearly rainfalls increasing since the 1970's according to (Bowman et al. 2001), that possibly explain a noticeable trend of rising woody biomass.

Apart from transitions in rainfall events, atmospheric CO_2 concentration plays also an important role in the wood encroachment of savannas. Naturally C4 grasses hold an advantage in savanna ecosystems over the C3 tree species. They feature a specialist mechanism to increase the CO_2 concentration in cells of the thylakoid membrane that perform the light reaction of photosynthesis and thereby reduce the rate of photorespiration that is a major limitation on photosynthetic efficiency at high temperatures. As the atmospheric CO_2 concentration increases, this specialist adaptation is less of an advantage as carbon saturation of the C4-photosynthesis takes place (Mitchard & Flintrop 2013; Scheiter & Higgins 2009). Trees will take advantage of the lower pressure from the grasses and will seize the opportunity to grow more saplings and cover larger areas (Scheiter et al. 2014; Bowman et al. 2001). This will affect the tree-grass ratio of the savanna substantially. It is therefore important to gain understanding of these changes of tree-grass ratio through time and the impacts they have on the dynamics and functioning of the ecosystem.

2.6 Remote sensing as a tool to monitor vegetation dynamics

2.6.1 Basics behind remote sensing

Field measurements have their limitations and do not allow the large-scale and frequent follow-up of vegetation dynamics. The advent of remote sensing, bringing important benefits with it as the systematic revisits, the spatial coverage and the ability to derive vegetation features from spectral information, allow to monitor the temporal and spatial dynamics of vegetative systems more intensely and with minimal environmental impact. Remote sensing is defined as the acquisition and measurement of information about an object or phenomenon without making physical contact with the feature under surveillance, and thus in contrast to on-site observation (Jones & Vaughan 2010; Khorram et al. 2012). Treasuring many advantages as it is a non-contact and non-destructive method of gathering information, this technique is more and more often applied in terrestrial ecology. Remote sensing encompasses technologies ranging from classical satellite remote sensing capturing large geographical areas to airborne sensing, right down to close-range remote sensing of individual structures or phenomena (Jones & Vaughan 2010).

Going into more detail into the physical aspect, this technique relies on the measurement of electromagnetic energy. Electromagnetic radiation consists of electromagnetic waves, which are synchronized oscillations of electric and magnetic fields that propagate at the speed of light through a vacuum. When a wavelength reaches an object it will interact with it as part of the signal will be transmitted through the object, part will be absorbed by the object and part will be reflected. This reflected signal can then be intercepted by a sensor. The law of conservation of energy states that the total amount of energy dissipated by reflection, transmission and absorption equals the incident energy. The human eye only responds to a small part of the electromagnetic continuum, called the visible (VIS) spectrum. This region corresponds to the photosynthetically active region (PAR) and stretches from 400 nm to 700 nm, which corresponds to the reflection of the violet-blue-green-yellow-orange-red light. On the shorter wavelength side the VIS is flanked by the ultraviolet (UV) region, ranging from 10 nm to 400 nm. The longer wavelength side of the VIS extends towards the near infrared (NIR from 700 nm to 1 μm), the mid-infrared (MIR from 1 to 4 μm) and the thermal infrared (TIR from 4 to 15 μm). This latter region is often referred to as the thermal region whereas the other regions all belong to the optical region (Jones & Vaughan 2010).

The quality of the sensing process of the reflectance signal depends heavily on the sensor and its spectral resolution, that is defined as the range of wavelengths that an imaging system can detect. Ranges can on the one hand be mentioned as the numerical wavelength interval, e.g. 450 nm to

495 nm, or can either be referred to as bands, which consists of a group of wavelengths, e.g. the blue band (Khorram et al. 2012). Increasing the spectral resolution, imaging systems can variate from simple broadband sensors, recording only the red, blue and green (RGB) bands, to multispectral sensors, capturing more than three bands, to hyperspectral sensors, capturing around 50 bands with a bandwidth of only a few nanometres (Jones & Vaughan 2010).

2.6.2.The typical vegetation spectrum

The reaction between the electromagnetic signal and any material creates a unique spectral response that provides information on the identity or condition of the feature and is therefore known as its spectral signature (Khorram et al. 2012). This explains why soil spectra differ from oceanic spectra or vegetation spectra, but also why the spectrum of an African baobab tree (*Adansonia digitate* L.) differs from the spectrum of an Australian boab tree (*Adansonia gregorii* F.M.). However all plant species share a basic format of spectral signature (Figure 2.2). This format is marked in the visible wavelengths by the chemical composition of the species, including photosynthetic pigments as chlorophyll, carotenoids, xanthophylls and flavonoids. The dominant pigments, chlorophyll a and b, account for almost all the absorption in the red wavelengths and the bulk of the blue wavelengths, resulting in the reflectance of a green signal. Carotenoids and xanthophylls cover the blue-green absorption spectrum and generate a yellow-orange visual signal. Absorption by the different pigments, enhanced somewhat by the internal scattering of radiation encountering air/water interfaces at the surface of cells with different refractive indices, generates a low reflectance signal. The NIR region is characterized by a high reflectance plateau due to the increased scattering within the cellular micro structure of the leaf. Moving to the short wave infrared (SWIR, 1.25 µm to 2.6 µm) region, strong water absorption bands dominate the gradually decreasing reflectance signal of green vegetation. Developments in the composition, e.g. leaf senescing or as a result of environmental stress, or micro structure, e.g. maturation or as a result of water stress, of leaves influence the visible spectrum, i.e. leaf colour, and the mid infrared spectrum respectively (Jones & Vaughan 2010).

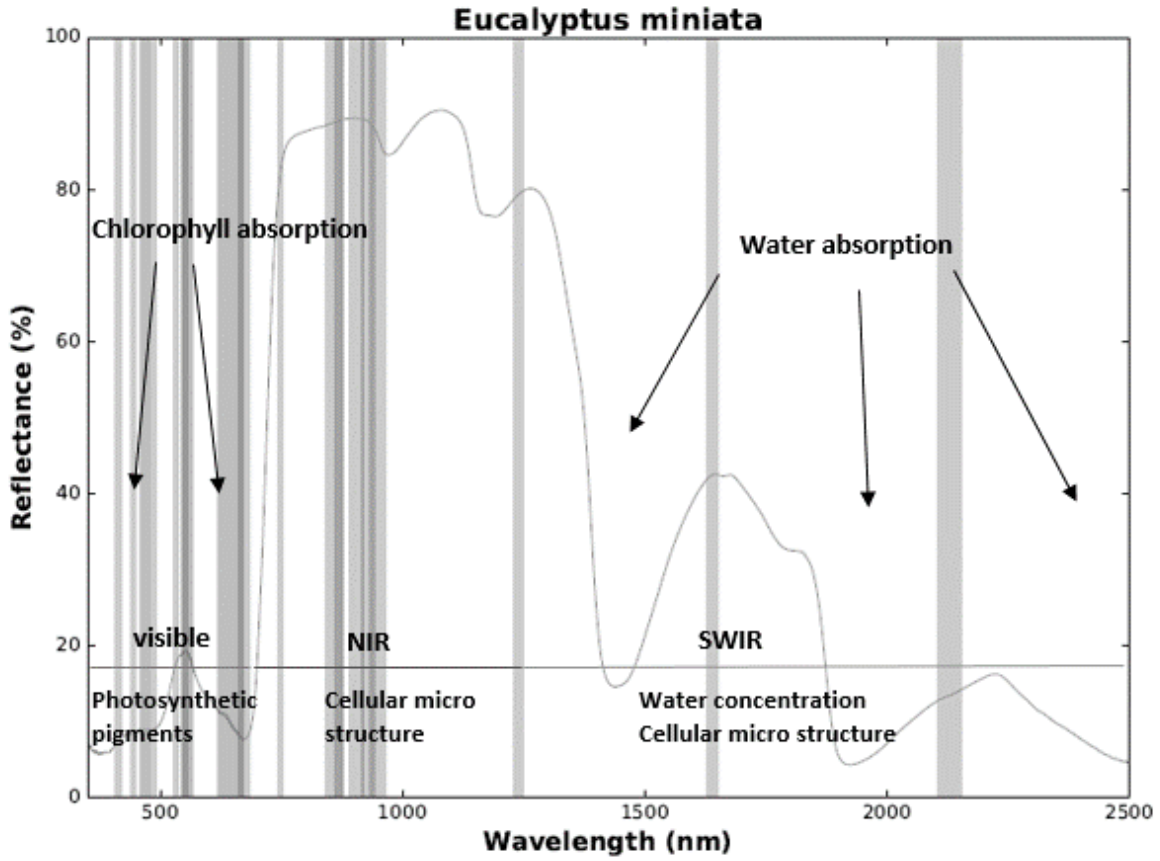

Figure 2.2: The typical format of a vegetative spectrum, here of an Eucalyptus miniata. The grey spectral bands mark interesting wavelengths in the visible, NIR and SWIR that are frequently used for vegetation indices. The chlorophyll pigment in plant leaves strongly absorbs visible light for use in the photosynthesis process, indicated by the two chlorophyll absorption arrows. SWIR light is greatly absorbed by the water concentration of the plant leaves and is visualized by the three water reflectance dips.

2.6.3 Monitoring vegetative systems

The spectral signature concept, introduced in previous paragraph, shows that the spectral signature of vegetation is defined by a set of biophysical parameters. The detection and calculation of these parameters happens through derivation of spectral band combinations that are known to be sensitive to these specific vegetation properties. The dimensionless measures that result from this are known as vegetation indices (VI) (Jones & Vaughan 2010). The abundance of VIs, especially present since hyperspectral remote sensing data became a standard element of vegetation monitoring, offered an immense range of band combinations (Mašková et al. 2008).

A well-known vegetation index that is able to distinguish vegetation surfaces from bare soil or water surfaces as well as indicate the vegetation health and greenness, is the Normalized Difference Vegetation Index (NDVI) (Rouse et al. 1973). This index utilizes absorption by chlorophyll in the red

wavelength and scattering by cellulose in near-infrared wavelengths to indicate greenness of vegetation (Guerschman et al. 2009). Healthy vegetation absorbs most of the VIS wavelengths that hit the plant and reflects a large portion of the NIR radiation. In case of unhealthy vegetation, the difference between reflected radiation of the NIR and VIS wavelengths is lower as there is less visible light absorbed and less NIR radiation reflected. NDVI values range between -1 and +1 for all natural surfaces whereby values increasing from 0 to 1 correspond to increasing density of green/healthy leaves. Here one can also conclude that lower values above zero can coincide with sparser vegetation types like tundra, desert or grassland. Values below zero correspond with water surfaces.

The repetitive acquisition of satellite imagery enables the establishment of time series of vegetation indices which allow to detect, quantify and characterize dynamics, changes and trends of biophysical processes over time (Lhermitte et al. 2011; De Keersmaecker et al. 2015). The spatial, spectral and temporal characteristics of the remote sensing data determine the performance of this time series analysis (Lhermitte et al. 2011). The temporal variation in NDVI is frequently used to characterize the phenological dynamics as it indicates when vegetation is sprouting, maturing or wilting in time. Time series of NDVI feature typically three main parts: (i) a seasonal component with a vegetation specific amplitude, timing and shape, related to the phenology of the vegetation, (ii) trends, which are gradual changes over time, and (iii) the anomaly, defined by the short-term response of vegetation biomass to environmental anomalies such as a drought period and noise (De Keersmaecker et al. 2015; van Rooijen et al. 2015). According to Verbesselt et al. (2010) and Lhermitte et al. (2011) phenological cycles may alter over the years which may be both associated with (i) gradual changes, i.e. interannual changes due to climate variability or gradual changes in land management/degradation, and with (ii) seasonal changes, driven by interactions between annual temperature and rainfall impacting plant phenology, or (iii) abrupt changes, caused by environmental disturbances.

2.7 Remote monitoring of woody cover

Given the increasing interest in the future vision of savanna ecosystems regarding the woody thickening phenomenon, several studies have examined the evolution of woody cover through time. Woody cover is in this research study defined as the projection of woody canopies on the ground surface. The NDVI, as a greenness indicator, is therefore often used as a proxy to estimate this mean foliage density of the present vegetation (Brandt et al. 2016). Highlighting however only the woody cover layer with the NDVI as a proxy is not always evident considering the vegetation structure of this ecosystem. This tropical savanna ecosystem is namely characterized by the tight relationship between the herbaceous understorey and the upper woody layer. Segregating both layers from a satellite image

based on the NDVI is not that easy as the NDVI gives only an indication of the greenness or healthiness of the vegetation. In this case, the outspoken dynamic seasonal character of this ecosystem offers the solution. While the tree layer might stay green and thus photosynthetically active the whole year through, the herbaceous understorey is solely abundant during the wet season and shows its senescence shortly after flowering towards the last rains. This makes the dry season the most suitable timing to estimate woody cover using satellite imagery.

Over the years a trend has established to estimate woody cover percentages with high spatial resolution earth observation data like Quickbird (Rasmussen et al. 2011) or WorldView-1&2 (Karlson et al. 2014; Brandt et al. 2016). However the benefits from obtaining results at a few meters resolution are countered by the huge amount of data storage that is required, by the fee they charge to access these data and the fundamental question whether the analysis of a few images is representative for the continuous change of a highly dynamic ecosystem. In a study about the tiger bush in northern Senegal Rasmussen et al. (2011) used the eCognition software on Quickbird data to perform an object-oriented classification to assess tree cover. This classification technique delineates and classifies the image into homogeneous patches based on spectral and spatial parameters as well as user defined functions regarding shape, texture, context and spectral information. Given the disadvantages of high spatial resolution imagery, opting for high temporal but low spatial resolution earth observation time series of plant phenology or NDVI seasonal metrics can be considered more appropriate for this research study (Brandt et al. 2016).

In literature there are however a lot of studies found that also made use of aerial photography to tackle the assessment of woody canopy cover. Weisberg et al. (2007) used the eCognition software to perform an object-oriented classification on orthophotos from 1966 to 1995 to distinguish a certain tree type from the rest of the vegetation. Both Fensham et al. (2002) and Carreiras et al. (2006) made use of aerial photos to estimate woody canopy cover and overlaid them with a transparent grid of crosses or points respectively. Going over all the crosses/points the percentage of woody cover could be assessed as the number of tree crown crosses/points divided by the total number of grid crosses/points. There is however a risk of overestimation associated with this aerial photography technique that increases with decreasing scale of photography. Carreiras et al. (2006) approach was not only to estimate canopy cover based on aerial photography but compare this method with ordinary least squares linear regression models that make use of several indices including NDVI. In a study about the Kakadu National Park in Australia (Lehmann et al. 2009) tree cover was assessed using georeferenced digitized aerial photography from the years 1964, 1984 and 2004, and a stereoscope. The analysis gave satisfying results with an average of 62.7 % in 1964 and 67.6 % in 2004.

Concluding from the recommendations made in this subsection and given the interests of this research study, it is better to opt for high temporal resolution imagery instead of high spatial resolution images. Furthermore the outspoken seasonality of this dynamic ecosystem provides a tool to ease the distinction between the woody overstorey and the herbaceous understorey. Brandt et al. (2016) used this knowledge and introduced the dry season index (DSI), a NDVI based metric, to estimate woody cover based on MODIS satellite imagery.

2.8 Stability of Ecosystems

Characteristic to each ecosystem is that they provide a number of ecosystem services that determine the habitability and attractiveness of places and landscapes. Tropical savannas are not only considered to be a rich source of diversity, they also have a prominent role in climate regulation both at local and global scale by sequestering carbon in trees, shrubs and soils (Sangha 2006). The increased stress put on an ecosystem by environmental and anthropogenic disturbances can cause abrupt changes in the functioning of the ecosystem and the provisioning of these services (Gosling 2013). As the impact of disturbances are either described by their magnitude, duration, frequency or their change over space and time, the stability of an ecosystem can be likewise expressed in different ways. The general concept of 'ecological stability' tries to capture different facets of the ecosystem dynamics and how ecosystems react to these disturbances. The overall ecological stability can be subdivided in five main components, enlightening each their own vision on the concept of stability (Figure 2.3). As a measure of susceptibility, persistence gives an indication of how long a system maintains the same state before it changes in a certain direction (Donohue et al. 2016). Resistance is identified as the tendency of the system to remain close to its equilibrium state and withstand the environmental disturbance (Complexity Academy 2016) and is frequently measured as the dimensionless ratio of some ecosystem variable measured after, compared to before some disturbance event (Donohue et al. 2016). Resilience expresses the rate at which an ecosystem recovers after the disturbance (van Rooijen et al. 2015; De Keersmaecker, Lhermitte, et al. 2015). Robustness is a particular measure of resistance focused on the composition of the community. And at last, variance is the inverse of stability and is measured as the variability over space or time (Donohue et al. 2016).

a) b)

Figure 2.3: Schematic representation of the five main components of ecological stability, here used in an example with the biomass development of trees over time (Adapted from Donohue et al. 2016).(a) In the first situation the total tree biomass shows a small dip after which the ecosystem slowly recovers which results in a change of some tree species. This explains the high resistance, low resilience and moderate persistence. As the recovery of the biomass is successful, robustness is high. After recovery there is still some small variability in biomass present; (b): The second situation shows a larger decrease in total biomass, resulting in a low resistance. The system recovers however faster and shows thus a higher resilience. There is no loss or change in tree species which corresponds to a high robustness and high persistence. After recovery though, there remains some higher variability in tree biomass.

2.9 Quantification of vegetation resilience

When disturbances take place, the ecosystem gets pulled out of its normal operating parameters. The system can either recover or it can lead to a tipping point at which a sudden shift in the dynamical regime takes place. In a study of Scheffer et al. (2009) a review is given on all sorts of indicators that act as early-warning signals for reaching critical transitions in certain scenarios. The most important and straightforward clues that have been suggested as indicators of whether a system is approaching a critical threshold are related to a phenomenon known in dynamical systems theory as 'critical slowing down' (Wissel 1984). As the pace of the system is critically slowing down, the recovery rate is decreasing smoothly to zero as well when getting close to the critical threshold which leads to an overall increasing recovery time from disturbances (Scheffer et al. 2009; Dai et al. 2015). This implies that the recovery rate after a disturbance event is a first indicator of how close a system is to the tipping point. A second indicator follows from the fact that slowing down causes the intrinsic rates of change in the system to diminish whereby the state of the system at any moment of time resembles more and more to the previous state. This translates itself in an increasing autocorrelation trend towards the critical transition point. The most straightforward calculation is the lag-1 autocorrelation, which can be directly interpreted as slowness of recovery. Slowing down not only causes an increasing autocorrelation signal but also a noticeable, increased variance in the pattern of fluctuations. Besides the critically slowing down process, other indicators regarding the asymmetry, and skewness also reveal how far the system is from the tipping point (Scheffer et al. 2009).

2.10 Scope of this master thesis research

In this master thesis research the highly dynamic tropical savanna ecosystem of northern Australia, being steered by climatic, biological and anthropogenic drivers, will be the subject of this study. More specifically, this study will focus on the woody cover dynamics of the system monitored through analysis of satellite observations, and investigate its influence on the ecosystem's short-term stability. To gain a deeper understanding of this relation, other influencing factors as bare soil coverage and fire frequency will also be looked in.

The specific research questions of this study are:

1. Quantifying woody cover dynamics:
   How is woody cover evolving over time in a tropical savanna ecosystem like Litchfield National Park from 2002 to 2016? Are woody thickening trends taking place in a tropical savanna ecosystem like Litchfield National Park?
2. Relation woody cover dynamics and short-term stability:
   Do woody cover trends have an impact on the short-term stability of this savanna ecosystem? What is the influence of other driving factors of the savanna ecosystem like fire events and fractional coverage of bare soil?

3 MATERIALS

3.1 Study area

The study area of this master thesis research is situated in the Litchfield National Park in the Top End geographical region of Australia (Figure 3.1). A total area of approximately 700 km² of the park covers an open-forest savanna region and is according to the Land Zones Tropical savannas map of Brocklehurst (2008) located on Mesozoic to Proterozoic rocks-ranges hills and lowlands. The site is situated in the northern mesic tropics that has a typical monsoonal climate with an intense summer monsoon season. The average annual precipitation ranges between 1200 mm and 1600 mm, falling almost entirely in the wet season from November to March (Australian Bureau of Meteorology 2007a). Temperatures are high in the region, with records of 1996-2005 showing maximum temperatures variating between 36 °C and 39 °C in September and October, while minimum annual temperatures range between 18 °C and 21 °C (Australian Bureau of Meteorology 2007b). As one of the main drivers of the savanna ecosystem, fire events determine to a large extent the landscape and its vegetation structure. According to Bushfires NT (Murphy et al. 2014), around 51% of the Litchfield National Park, which extends over an area of 1464 km², burns every year. Since the declaration of a National Park in 1986, controlled burning programs have been taking place at the beginning of the dry season in order to prevent major late dry season fires (Bowman et al. 2001).

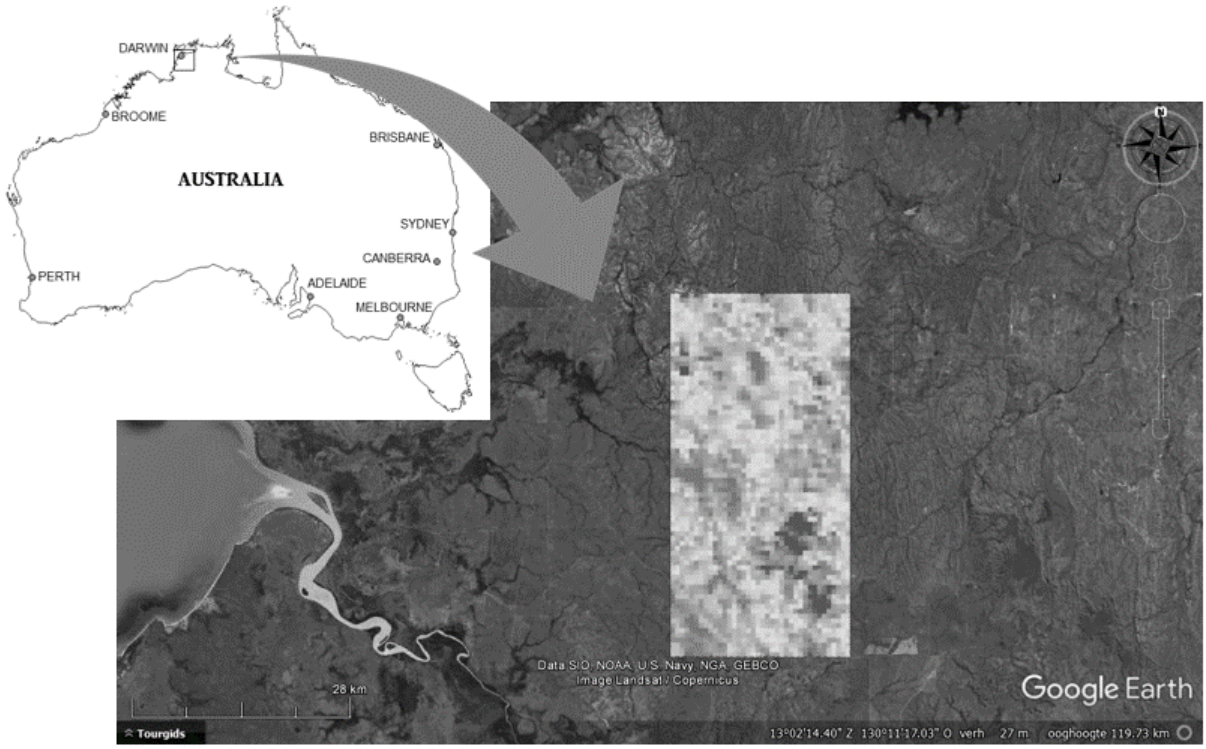

Figure 3.1: Location of the study area (boundaries: upper left corner: 13.0890 ° S, 130.7144 ° E, lower right corner: 13.5015 ° S, 130.9202 ° E), situated in the Top End of Australia. The study area is marked by the rectangle, filled with pixels that get a value according to the reflectance of the red band (620 nm – 670 nm) of the Moderate Resolution Imaging Spectroradiometer (MODIS) satellite.

3.2 Vegetation structure Litchfield National Park

This tropical savanna ecosystem within the Litchfield National Park is built up as a three layer mixture with an overstorey dominated by evergreen *Eucalyptus tetrodonta* and *Eucalyptus miniata*, a mid-storey of pan tropical semi- to fully deciduous tree and shrub species and an understorey dominated by C4 annual and perennial grasses (Hutley & Beringer 2011). Next the vegetation structure will be unravelled layer by layer and a brief overview of each of the layers will be given. A field study on site showed that the understorey is to a large extent dominated by perennial tussock grasses like *Sorghum plumosum*, *Heteropogon triticeus* and annual *Pseudopogonatherum* grasses (Simon 2010), interspersed with some herbaceous plants like *Cyperaceae sp*. (Reznicek 2008) and subshrubs as *Hibbertia brevipedunculata* (Cowie 2013). The mid-storey reveals a high diversity and can be seen as a patchwork of small shrub and tree species, palms and juveniles of *Eucalyptus tetrodonta* and *Eucalyptus miniata*. In this patchwork species like Grevillea (*G. pluricaulis* and *G. pteridifolia*) with their brightly coloured flowers are present, accompanied by a diversity of trees of the genus Acacia (*A. lamprocarpa*, *A. oncinocarpa, A. leptocarpa* and *A. tolmerensis*), that are known to have evolved some fire resistance, as well as *Buchanania obovata*, also known as wild mango (Cowie 2013). Zooming in on the overstorey, savannas above the 1200 mm isohyet are mostly dominated by *Eucalyptus miniata* and

Eucalyptus tetrodonta, as in this case. Both tree species belong to the larger eucalypts, reaching heights around 15 to 25 meters (Werner et al. 2008), and show adaptations to the prevailing dry environment susceptible to wildfires. *Eucalyptus tetrodonta*, also known as Darwin Stringybark, has a typical rough and compact, long fibred bark layer that persists to the smaller branches. *Eucalyptus miniata*, or Darwin Woollybutt, on the other hand has a short-fibred and somewhat stringy or flaky-papery bark layer that sheds from the upper part of the trunk and branches in papery flakes. As these two species hold more than 90% of the upper layer, *Erythrophleum chlorostachys* covers the other 10% (Boland et al. 2006).

3.3 Data

3.3.1 NDVI data (MCD43A4)

To quantify woody cover dynamics and their influence on the short-term stability, NDVI time series were created over the study area using imagery from the Moderate Resolution Imaging Spectroradiometer (MODIS) satellite. More specifically, data of the MCD43A4 product were used, a nadir Bidirectional Reflectance Distribution Function (BRDF) adjusted reflectance product with a spatial resolution of 500 m covering the VIS (459 nm – 670 nm), NIR (841 nm – 876 nm) and SWIR spectrum (1230 nm – 2155 nm) (Schaaf et al. 2002). Each 8 day composite selects the highest quality value from both Terra (overpass time 10 a.m.) and Aqua (overpass time 13 p.m.) satellites to minimize the influence of cloud coverage (Brandt, Hiernaux, Rasmussen, et al. 2016). The NDVI was calculated for the entire study area from November 2001 to September 2016 using the red band (620 nm – 670 nm) and NIR band (841 nm – 876 nm) of the MCD43A4 product (Frazier 2017). The NDVI is calculated as the ratio of the difference over the addition of the two bands (Rouse et al. 1973):

$$\text{NDVI} = \frac{\lambda_{NIR} - \lambda_{RED}}{\lambda_{NIR} + \lambda_{RED}} \quad (1)$$

With λ_{NIR} : the reflectance of the NIR band (841 nm – 876 nm)

λ_{RED} : the reflectance of the red band (620 nm – 670 nm)

In total 687 images, covering the whole study area, were collected for analysis and were reprojected from the sinusoidal coordinate system to the geographic coordinate system (° latitude, ° longitude) with WGS84 datum. Pixels with a low quality (based on fill values and magnitude inversion criteria of the MCD43A2 product) (Schaaf et al. 2002) for at least one of the two bands were masked out, which resulted in a data loss between 28.38% and 38.57% per pixel for the entire time series.

3.3.2 Surface cover data (MOD44B)

In order to gain a better understanding on the ecosystem short-term stability dynamics, additional datasets were consulted as possible explanatory factors. The percentage tree and bare soil cover within each pixel were extracted from the MOD44B product from 2002 to 2015, i.e. the Vegetation Continuous Fields (VCF) Yearly L3 Global product, having a spatial resolution of 250 m. The VCF product is produced using 16-day Land Surface Reflectance composites with a spatial resolution of 500 m, covering the Terra MODIS bands 1 to 7 (459 nm – 2155 nm), the Land Surface Temperature Data using MODIS bands 20 (3660 nm – 3840 nm), 31 (10780 nm – 11280 nm) and 32 (11770 nm – 12270 nm), and the MODIS Global 250 m Land/Water Map (Townshend et al. 2011). It contains proportional estimates of surface cover types such as tree cover, herbaceous vegetation and bare soil cover (Liu et al. 2015). These data were first reprojected from the sinusoidal coordinate system to the geographic coordinate system with WGS84 datum after which they were resampled to the same spatial resolution as the NDVI data (0.0055°), calculating the average value of surrounding pixels, in order to enable the comparison between the different datasets.

3.3.3 Burn data (MCD45A1)

As fire events are considered to have an important impact on the dynamics of the Australian tropical savannas (Beringer et al. 2015; Bristow et al. 2016), monthly burned area data were consulted as well. The algorithm of the MCD45A1 product with a spatial resolution of 500 m analyses Terra and Aqua MODIS derived daily Surface Reflectance inputs to locate rapid changes. With that information it detects approximate dates of burning and maps only the spatial extents of recent fire events and excludes fires that occurred in previous seasons or years (Boschetti et al. 2013). Burn date imagery of the product were collected from 1 January 2002 to 31 December 2016 on a monthly basis with lack of June 2001 (due to prolonged outage of the MODIS instrument). These data were converted to fire frequencies first per month and afterwards per year for the entire region. Afterwards these data were converted to WGS84 datum and were resampled to the same grid as the BRDF adjusted reflectance and VCF data in order to facilitate further calculations.

4 METHODS

4.1 Quantifying woody cover dynamics

In order to quantify woody cover dynamics in the Litchfield National Park, the Dry Season Index (DSI) was used. Tree cover products have been developed over time (e.g. MODIS) to estimate dense forests. Savanna ecosystems however consist of diverse patches of trees interspersed between a continuous layer of grasses, whereby an adapted approach is required to calculate accurately the woody cover changes. The DSI, developed by Brandt et al. (2016) for dryland in the Sahel, relates to the mean foliage density and serves as a proxy for woody cover.

The main rationale behind the DSI is the fact that grasses in the tropical Australian savannas wither during the dry season (Figure 4.1) whereby the NDVI signal is strongly determined by the woody cover, that stays green the whole year through. The main idea is therefore to use the dry season NDVI as a proxy for woody cover. Variations in water availability during the wet season though can cause fluctuations in greenness of the woody cover (and thus NDVI) during the dry season. Because such NDVI fluctuations are not directly corresponding to woody cover changes, a correction factor must be added.

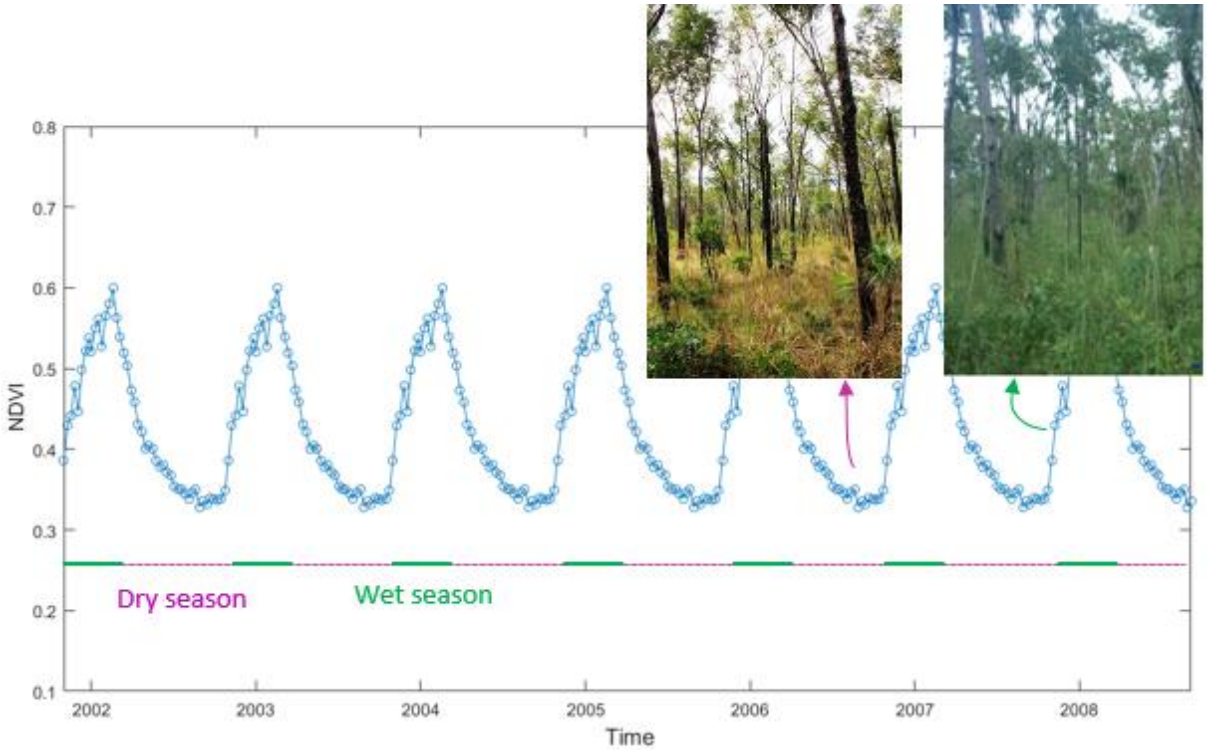

Figure 4.1: The seasonal pattern of the NDVI shows the growth dynamics over time. At the beginning of the growing period (start of the wet season) the NDVI curve will slowly increase which corresponds to the start of the seedlings growth. Next the signal goes over in a steep increase that will gradually flatten, coinciding with the time of maturation, and subsequently turn into a first slow and later sharp decreasing signal that expresses the withering phase of the herbaceous layer. This pattern can be related to the specific climatic conditions, which in this study show a stark division between the dry season (April – October) and the wet season (November – March).

Three main components are required to calculate the DSI: the mean dry season NDVI (proxy for the mean foliage density during the dry season), the wet season maximum NDVI (being a proxy for the growing conditions and vegetation heath state during the wet season) and the base level or mean annual minimum NDVI value (proxy for the minimum permanent leaf coverage) (Brandt, Hiernaux, Rasmussen, et al. 2016). Taking the temporal resolution of the MCD43A4 product into account, the dry season was set from 7 April to 24 October (or 6 April to 23 October in a leap year) and the wet season from 1 November to 30 March (or 31 October to 29 March in a leap year). Wet season data from 1 November 2001 to 30 March 2002 were attributed to the DSI calculation of 2002 given the fact that three of the five months are situated in 2002.

First of all a smoothening was performed on the wet season parts of the NDVI time series. Due to a higher cloud cover during the rainy season a high percentage (66.25% - 87.50%) of the pixels were flagged as having a low quality value and were therefore masked. To reduce the number of these missing and residual low quality values, a running mean over 5 images was calculated. After smoothening, the mean dry season NDVI was derived for each year, serving as a proxy for the mean foliage density over the dry season.

Yet inter-annual variability in growth conditions during the wet season may cause fluctuations in dry season NDVI that are not related to changes in woody cover. For example, a larger water availability during the wet season may result in a larger dry season NDVI while woody cover remains the same. Hence, the dry season NDVI should be corrected for this interference. If a significant linear relationship ($p < 0.05$) between the wet season maximum NDVI and the following mean dry season NDVI was present, the dry season NDVI was corrected using a correction factor. This correction factor consists of the difference between the predicted dry season NDVI (using the linear regression between dry and wet season NDVI) and the reference season, represented as the mean peak over the whole time span.

The minimum permanent leaf coverage without any green herbaceous influence was ensured by calculating the mean annual minimum dry season value. By including this component, singular major events, e.g. a wildfire but also remaining sensor noise and missing data caused by clouds, were attenuated. Piecing all these components together, the DSI was calculated as follows:

$$DSI = (DS\ actual + (reference\ DS - predicted\ DS) + base\ level\ DS)/2 \quad (2)$$

With DS actual referring to the mean dry season NDVI, reference DS to the mean peak over the whole time series (15 years), predicted DS to the linear regression between mean dry season NDVI and wet

season maximum NDVI, and lastly base level DS corresponding to the mean annual minimum NDVI. In case no significant linear relationship between the mean dry season NDVI and the wet season maximum NDVI was found, the DSI was calculated without the correction factor as follows:

DSI = (DS actual + base level DS)/2 (3)

As a final step, a running mean over 2 years (averaging the current and the previous year) was applied on the DSI time series to minimise uncertainties caused by data gaps introduced by missing data or the masking of low quality data (Brandt et al. 2016). The final DSI results are an estimation of the woody cover with high DSI values corresponding to a high woody cover and low DSI values to a low woody cover.

After calculating the DSI, an analysis of (i) spatial patterns in woody cover and (ii) temporal woody cover changes was performed. Spatial patterns in woody cover were explored using the average DSI and its inter-annual variability over the total time span of the DSI time series (2001 to 2016). Moreover, in order to gain insight in differences between the DSI and existing tree cover products, the average and inter-annual variability of the DSI and VCF tree cover were compared. In order to define if significant relationships were present between both variables, correlation tests were executed at the pixel level. Evaluation with the t-statistic stated the relevance of these correlations based on a significance threshold of 0.05. Subsequently, temporal woody cover changes were quantified using a linear trend analysis on the DSI time series.

4.2 Short-term stability

NDVI time series can be split up in three main parts: (i) a seasonal component with a vegetation specific amplitude, timing and shape, related to the phenology of the vegetation and the environmental conditions, (ii) trends, which represent the gradual changes over time, and (iii) the anomaly, defined by the short-term response of vegetation biomass to environmental anomalies such as a drought and noise (De Keersmaecker et al. 2015; van Rooijen et al. 2015). In order to characterize the short-term vegetation response (stability) of this savanna ecosystem, the anomaly component needed to be extracted from the NDVI signal. A first step was therefore to reconstruct the seasonality by taking the mean NDVI value for each day of the year. After subtracting this seasonality component from the NDVI signal, the data were detrended, if significant trends ($p<0.05$) were present, resulting in the anomaly component of the NDVI signal. Figure 4.2 and 4.3 give a representation of this decomposition process.

Two stability indicators were subsequently derived from the NDVI anomaly time series: the vegetation variance and the vegetation resilience to climate anomalies. Firstly, vegetation variance was defined as the standard deviation of the NDVI anomaly signal. Higher absolute values of the standard deviations correspond to higher fluctuations, or climate anomalies, over time, whereas lower absolute values indicate that the data points tend to be close to the average value of the time series. From an ecological perspective it can therefore be said that high standard deviations point to a higher susceptibility of the system towards changes or climate anomalies. Secondly, the autocorrelation at lag-1 was calculated to define the speed of the recovery rate or vegetation resilience of the system. The autocorrelation at lag-1 is a metric that measures the relationship between a variable's current value and its past values, and thus how much they are related. The size of the absolute value is in line with the traditional correlation, saying that higher absolute values indicate a higher resemblance (in case of a positive value)/perfect contrast (in case of a negative value) between the two time series. At an ecological point of view it can thence be understood that higher positive autocorrelation values indicate a slower recovery after a disturbance or change and thus a lower vegetation or ecosystem resilience.

Next to deriving the two stability metrics over the entire time span in order to assess the short-term stability of this savanna ecosystem and its drivers, stability changes were assessed by comparing changes in the stability metrics over the first (November 2001 - December 2008) and second half (January 2009 - September 2016) of the time series. Subdividing these results in positive and negative changes and combining both indicators allowed to make a division in four classes according to the overall trends: (1) both autocorrelation and standard deviation increase between the two time periods, (2) the autocorrelation decreases and the standard deviation increases, (3) the autocorrelation increases and the standard deviation decreases, and (4) both indicators decrease.

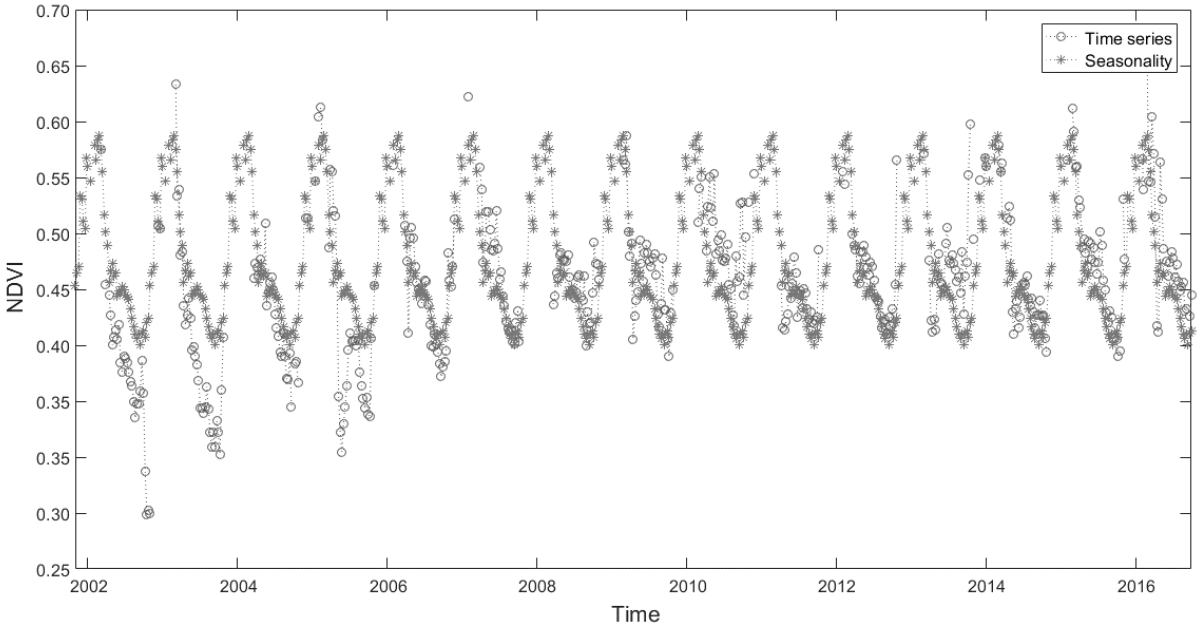

Figure 4.2: An NDVI time series for pixel (13.1715 °S, 130.7630 °E), masked for low quality values, and its seasonality component, calculated as the mean NDVI value of every day of the year. There is a striking difference in presence of data points between the wet and dry season noticeable.

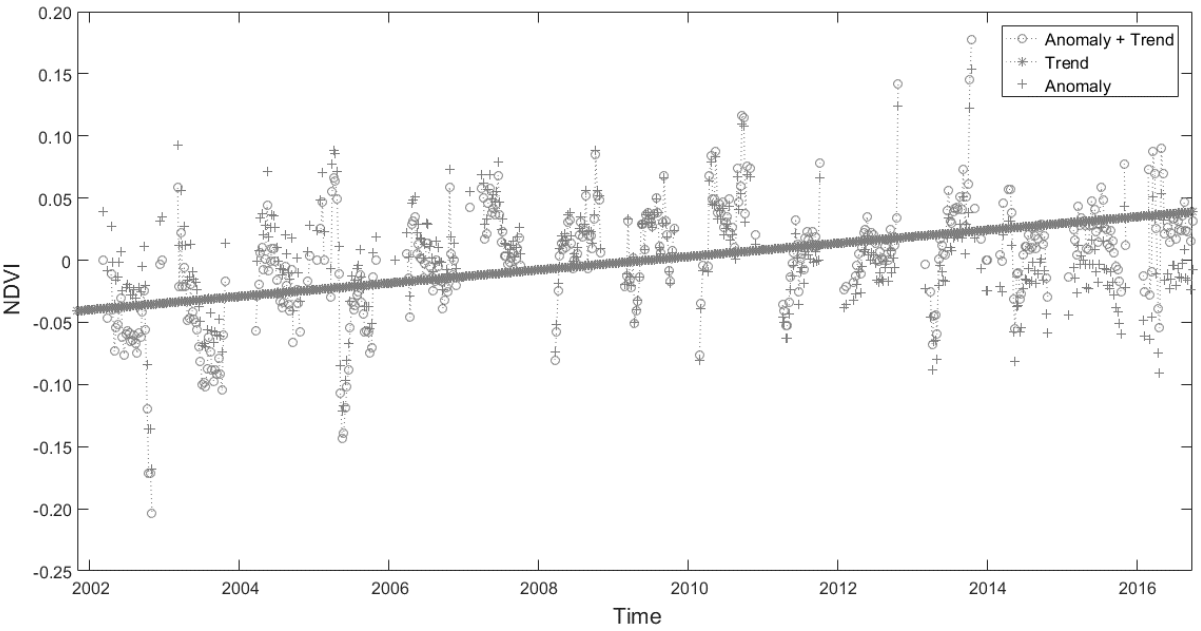

Figure 4.3: Further decomposition of the anomaly and trend components of the NDVI time series of pixel at 13.1715 °S and 130.7630 °E, masked for low quality values. In this case, a significant positive trend needed to be subtracted from the already deseasonalized NDVI signal to highlight the anomaly signal.

4.3 Linking woody cover and ecosystem's short-term stability

The objective of this master thesis research is to investigate if and in what way woody cover dynamics influence the short-term stability, or more specifically the vegetation resilience and variance, of the Australian savannas. As mentioned in the literature review, this ecosystem knows more ecological

drivers than just woody biomass growth. That is why not only woody cover dynamics were taken into account but also the impact of bare soil and fire events. Both spatial and temporal comparisons were made between all the different datasets.

Again, correlation tests were conducted between the two short-term stability metrics and the average DSI over time, the average bare soil cover over time and the total frequency of fire events to compare temporal variations at the pixel level. Secondly, in order to identify the determining factors of the short-term stability indicators, a multivariate linear regression analysis was performed on both stability indicators as response variables and with the average DSI, the average bare soil coverage and the total frequency of fire events as predictor variables:

$$\text{Stability} = \beta_0 + \beta_1 * \text{DSI} + \beta_2 * \text{Fire Frequency} + \beta_3 * \text{Bare Soil} \quad (4)$$

With Stability: the autocorrelation or standard deviation of the NDVI anomaly

- *β_0: the estimated intercept*
- *β_1: the estimated regression coefficient of the DSI*
- *β_2: the estimated regression coefficient of the fire frequency*
- *β_3: the estimated regression coefficient of the VCF bare soil cover*

In order to prevent correlated results, a systematic sampling strategy was applied that selected one pixel out of every 5 x 5 subsample in the total study area and was repeated 25 times. Histograms of the significant estimates and the total Root Mean Square Error (RMSE) of the model were plotted and the mean values were calculated. Given the mutual variability in significance, percentages of repeats with a significant p value were provided for each predictor variable.

To assess the effect of multicollinearity in this model, the variance inflation factor (VIF) was calculated. Multicollinearity occurs when predictor variables are highly correlated with other predictor variables, which complicates the eventual interpretation of the results of the model. This VIF is calculated as follows:

$$\text{VIF}_i = \frac{1}{1-R_i^2}$$

With R_i^2 the coefficient of determination from a regression of predictor i on the remaining predictors. A VIF of one corresponds to no multicollinearity among the predictor variables (Martz 2013). When the variation of a predictor is on the other hand largely explained by a linear combination of the other predictors, R_i^2 is close to 1, and the VIF for that predictor is correspondingly large. Generally there is a

threshold set that a VIF between 1 and 5 corresponds to moderately correlated predictor variables. If the VIF exceeds 5, there exists a real problem of multicollinearity as predictor variables are highly correlated and so the model contains redundant variables.

To observe the temporal stability changes and its determining factors, a multinomial logistic regression analysis (Krishnapuram et al. 2005) was performed on the categoric stability change classes (i.e. using four classes indicating combined increases and decreases in autocorrelation and standard deviation) with the DSI, burn frequency and VCF bare soil coverage as predictor variables. Characteristic to a multinomial logistic regression is that the response variable is expressed as a comparison of the categories (classes) to one reference category. As there are four categories in this case, three linear relationships will be calculated with the three categories over one reference category as response variable. The estimates of these relationships express the effects of the predictor variables on the log odds of being in one category versus the reference category. A positive value of one of the predictor variables indicates that the probability of being in the first category is the exponential of that positive value higher than being in the reference category, whereas negative values express a higher probability to be situated in the reference category. Here the reference category was set as the negative trends for both short-term stability metrics. Again the systematic sampling strategy was applied that selected one pixel out of every 5 x 5 subsample in the total study area and was repeated 25 times.

5 RESULTS

5.1 Woody cover estimation

Woody cover estimations based on the DSI calculation were made at an annual scale for the years 2002 to 2016. The next subsections aim for a deeper understanding and better view on the spatial patterns and temporal changes in woody cover of the Litchfield National Park.

5.1.1 Spatial patterns

Over the total spatial extent of the study area in Litchfield National Park, the average estimated woody cover (2002–2016) varies between a DSI of 0.2461 and 0.5685 with an overall mean DSI ($\pm$ standard deviation) of 0.3794 $\pm$ 0.0168. At first sight there are two patches visible with higher woody cover, one in the mid to south west border and one at the top in the middle (Figure 5.1, a). Woody cover in these areas ranges roughly between a DSI of 0.45 and 0.55 with the maximum coverage at 13.4135 °S, 130.7792 °E. The two zones are separated by a passage of lower woody cover that starts at the north west corner and proceeds to the mid to south east corner. The area with the least amount of woody coverage is situated at 13.4410 °S, 130.8926 °E. Looking at the variability of the DSI over the years (Figure 5.1, b), values fluctuate between 0.0057 (1.50% of the mean DSI) and 0.0450 (11.86% of the mean DSI). Areas with the highest inter-annual variability in DSI are situated around the 13.14 °S latitude.

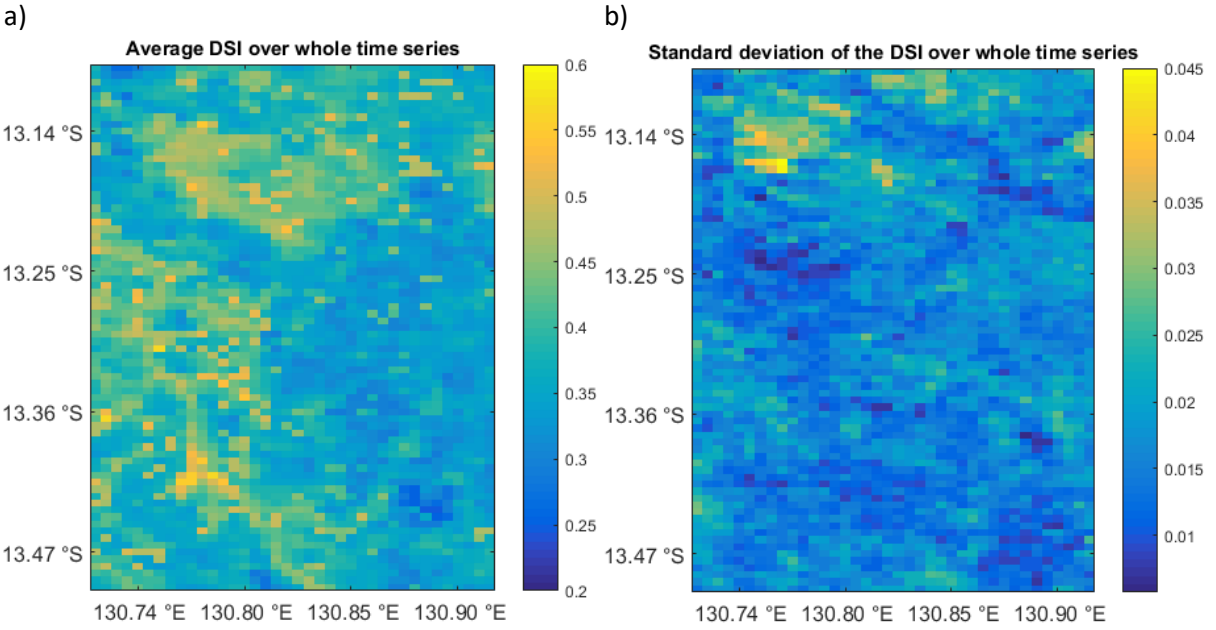

Figure 5.1 (a): Average DSI values for the total study area over the years 2002 to 2016. The higher the DSI, the higher the woody cover percentage; (b): The standard deviation gives a representation of the variability of the DSI over time. Lower values indicate small fluctuations over the years, whereas higher values indicate larger fluctuations.

5.1.2 Comparison with VCF tree cover product

The average tree cover over the 2002-2015 time span derived from the VCF tree cover product shows spatially similar patterns to the DSI (Figure 5.2, a). An overall average tree cover percentage is estimated at 10.83% $\pm$ 3.55%. Focusing on the standard deviation term (Figure 5.2, b), the spatial patterns here differ greatly from the DSI estimated inter-annual variability. Whereas they did not show many differences in the previous situation, they show now a spatial pattern that almost completely follows the DSI and VCF tree cover patterns. Areas where woody cover and tree cover are higher correspond to areas with a standard deviation varying roughly between 0.72% (6.65% of the mean VCF tree cover) and 9.00% (83.10% of the mean VCF tree cover).

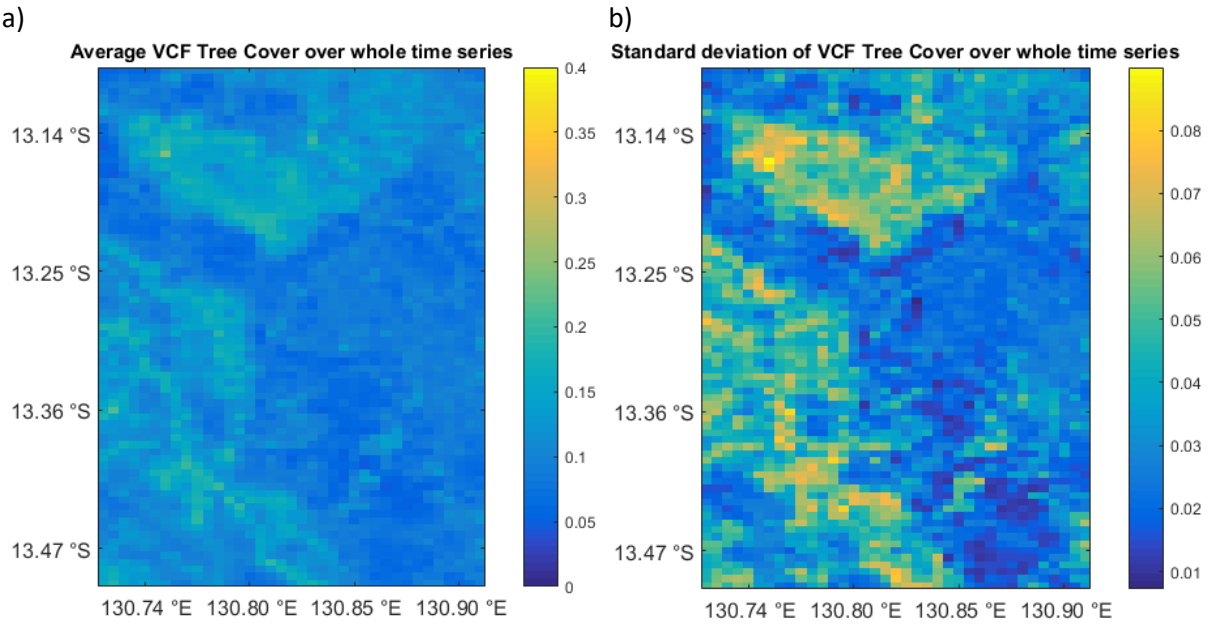

Figure 5.2 (a): Average tree cover values, according to the MOD44B VCF MODIS product, for the total study area over the years 2002 to 2015. Together with the bare soil cover product and non-tree cover product, they sum up to 1, corresponding to 100% coverage; (b): The standard deviation gives a representation of the variability of the tree cover over time. Spatial patterns resemble greatly to the spatial patterns of the DSI (see Figure x, a) and tree cover product.

The average DSI woody cover estimation and the average VCF tree cover product show a significant positive correlation over the years with a coefficient of 0.47. The scatter plot and the histograms of both woody cover estimations are presented in Figure 5.3.

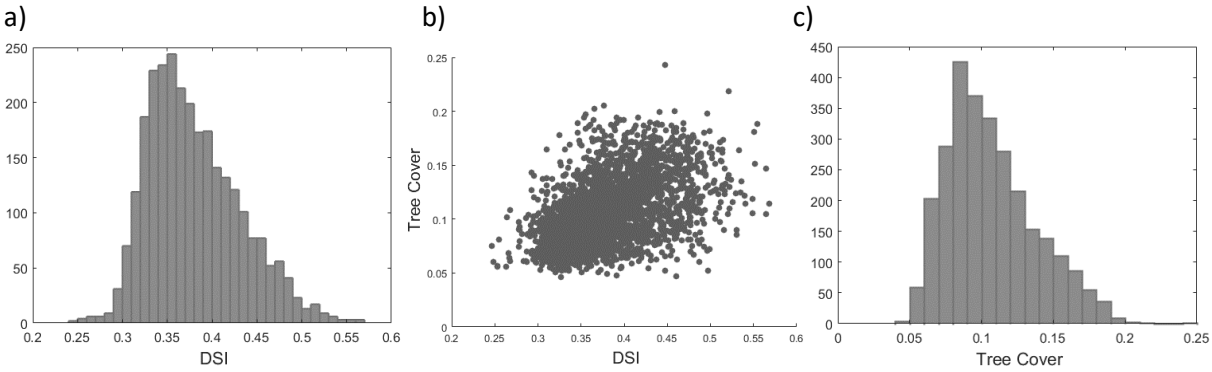

Figure 5.3 (a): The histogram of the average DSI from 2002 to 2016; (b): Plotting the average VCF tree cover product and the average DSI displays a positive relationship between both variables with a correlation coefficient of 0.4741 (p = 1.50E-155); (c): The histogram of the average VCF tree cover product from 2002 to 2015.

5.1.3 Temporal patterns

Trend analysis of the DSI woody cover estimations shows for some pixels a clear trend from 2002 to 2016 (Figure 5.4). The highest R^2 values (Figure 5.4, a) are located in the centre of the region with the maximum value of 0.8864 at 13.3255 °S, 130.8278 °E. Most of the trends (Figure 5.4, b) show small increments to maximally a DSI of 0.0087 (2.29% of the mean DSI), whereas some single pixels and clusters around the 13.14 °S and 13.36 °S latitude show very small decreasing trends up to a DSI of -0.0052 (1.37% of the mean DSI).

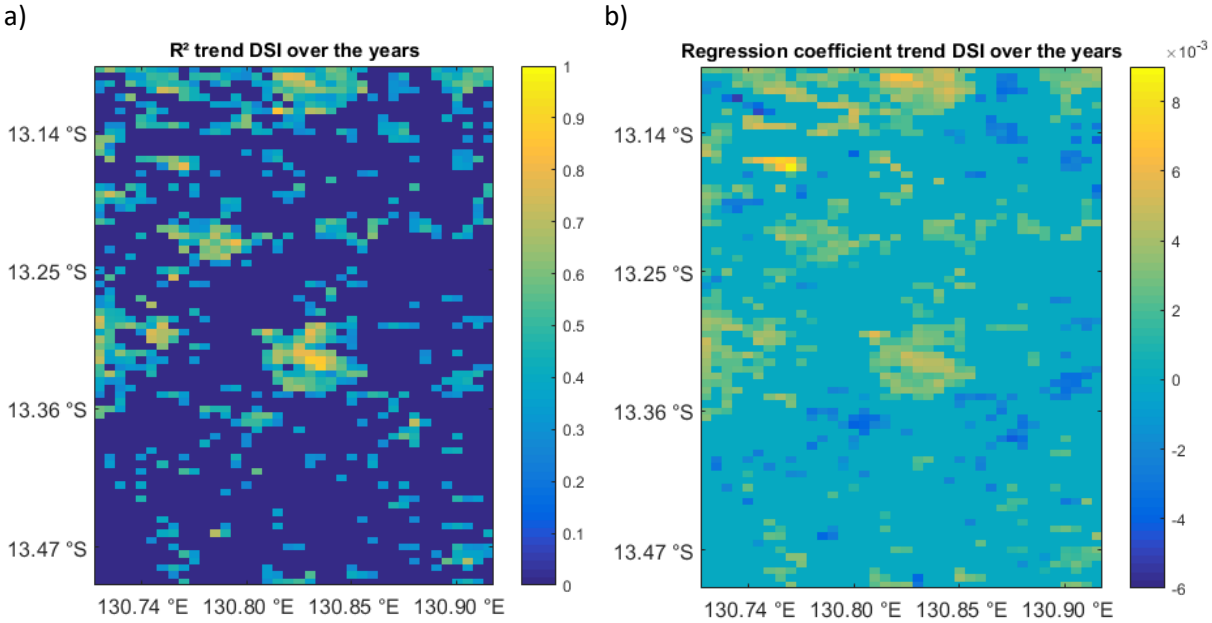

Figure 5.4 (a): The R^2 values are plotted in case a significant trend of the DSI between 2002 and 2016 was present. At first sight there are more significant trends present in the upper parts of the study region; (b): The regression coefficients of the trends are plotted in case a significant trend of the DSI between 2002 and 2016 was present. Positive values indicate an increment in woody cover over time whereas negative values correspond to a decrease.

5.2 Short-term stability

The short-term stability of the Litchfield National Park savanna ecosystem is in this study described by the autocorrelation and standard deviation of the anomaly signal of the NDVI time series from November 2001 to September 2016. Spatial patterns and temporal changes of both stability indicators are assessed in this subsection.

5.2.1 Autocorrelation

The autocorrelation at lag-1 of the NDVI anomaly - a first measure of the short-term stability - shows values fluctuating between 0.504 and 0.892 (Figure 5.5) with an average value of 0.788. In the study area there are four spots that reveal a higher autocorrelation: a minor cluster in the north (A), a larger patch a bit more south (B), a more diverse patch in the south west corner (C) and lastly a large area on the eastern border (D). These high autocorrelation values point to a slow recovery of the vegetation after possible disturbance events given that the similarity between the current and past NDVI anomaly is high. These areas have thus a low resilience. Autocorrelation values below the average value, corresponding to regions with a faster recovery speed and so a higher resilience, are situated in the north west to south east diagonal of the study area.

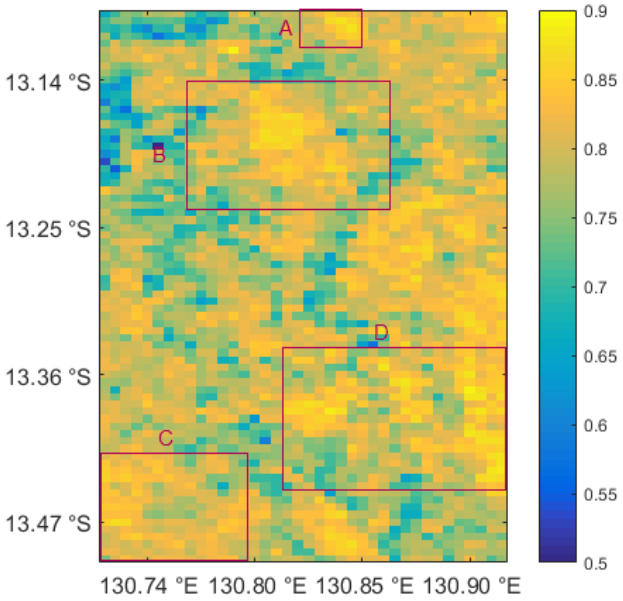

Figure 5.5: The autocorrelation of the NDVI anomaly time series is used as an indicator of the resilience of the savanna system. The higher the autocorrelation, the lower the resilience of the ecosystem as it corresponds to a longer recovery time.

5.2.2 Standard deviation

The standard deviation of the NDVI anomaly - a second indicator for the short-term stability of the system - varies between 0.024 and 0.060 with an overall average value of 0.040 for the total area. Figure 5.6 displays three spots (region A, B and C) with a higher standard deviation, revealing that the vegetation in these regions is more susceptible to disturbance or change events and as a consequence reacts stronger than less susceptible areas. Region B is surrounded by a cloud of lower standard deviations that merge in the centre of the image and follow a trail to the south east corner. This means that the vegetation in these areas is less susceptible to climate anomalies. Region D is this time characterized by above average standard deviations but does not show maximal values as for the autocorrelation.

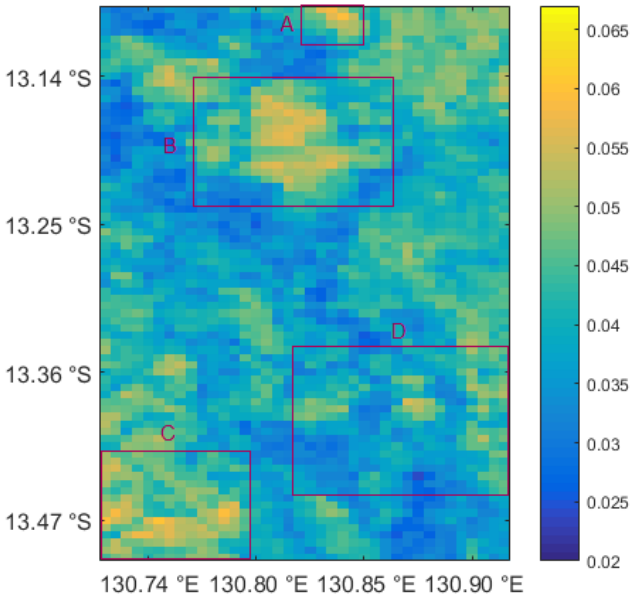

Figure 5.6: The standard deviation of the anomaly signal of the NDVI time series is a second metric for the short-term stability of the study region. The higher the standard deviation, the higher the temporal NDVI anomaly fluctuations and so the more susceptible the vegetation is in that area to disturbances.

5.2.3 Comparison short-term stability metrics

When comparing the autocorrelation (Figure 5.5) and standard deviation (Figure 5.6) of the NDVI anomaly signal, similar spatial patterns appear for both metrics. Yet, differences can be noticed on the eastern side of the study area (region D). Autocorrelation scores fairly high, indicating that it takes a lot of time for the vegetation to recover after disturbance events or changes. The standard deviation on the other hand shows no maximum values, indicating that the vegetation in this region is less susceptible to changes or disturbances than in the areas A, B or C. The high spatial comparison translates itself in a high positive correlation coefficient of 0.68 between the two short-term stability indicators (Figure 5.7).

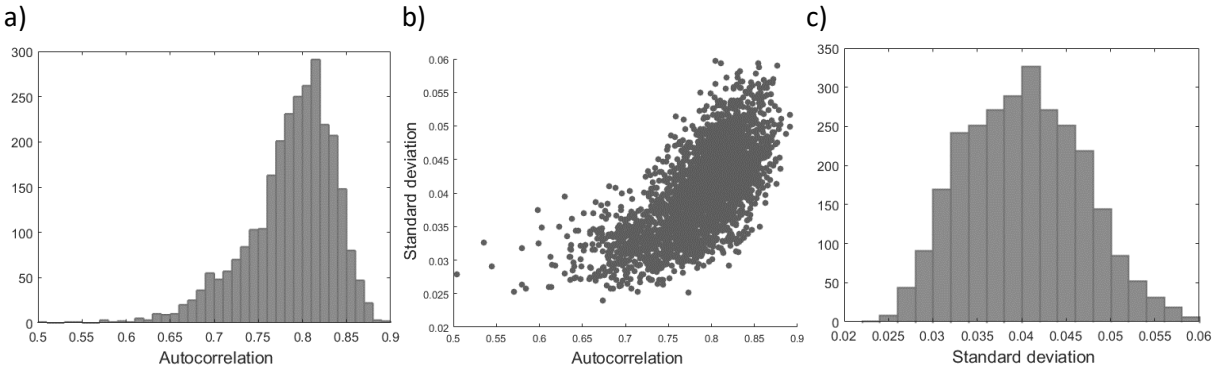

Figure 5.7 (a): The histogram of the average autocorrelation from November 2001 to September 2016; (b): Plotting the average autocorrelation versus the average standard deviation displays a high positive relationship between both variables with a correlation coefficient of 0.6765 (p = 0); (c): The histogram of the average standard deviation from November 2001 to September 2016.

Splitting up the data in the first (November 2001 – December 2008) and second half (January 2009 - September 2016) of the time series in order to observe temporal stability changes, and calculating the difference between both, results in an overall increasing trend of 0.0152 for the autocorrelation (Figure 5.8, a) and 0.0043 for the standard deviation (Figure 5.8, b). An increase in autocorrelation corresponds to a slower recovering vegetation and makes it therefore more susceptible to changes or disturbances. The increasing standard deviation confirms this hypothesis as it indicates a higher susceptibility and/or stronger reaction of the vegetation. Patterns for the autocorrelation show diverse patches that increase over the second half of the total time span with the highest increases on the east side of the study area at a latitude of 13.16 °S and 13.42 °S. The standard deviation of the NDVI anomaly signal shows also most increases at the 13.16 °S latitude as well as around the 13.36 °S latitude. Notable decreases in the autocorrelation and standard deviation, corresponding to a more resilient and less susceptible ecosystem respectively, are located mostly on the west side and the south east corner of the study area.

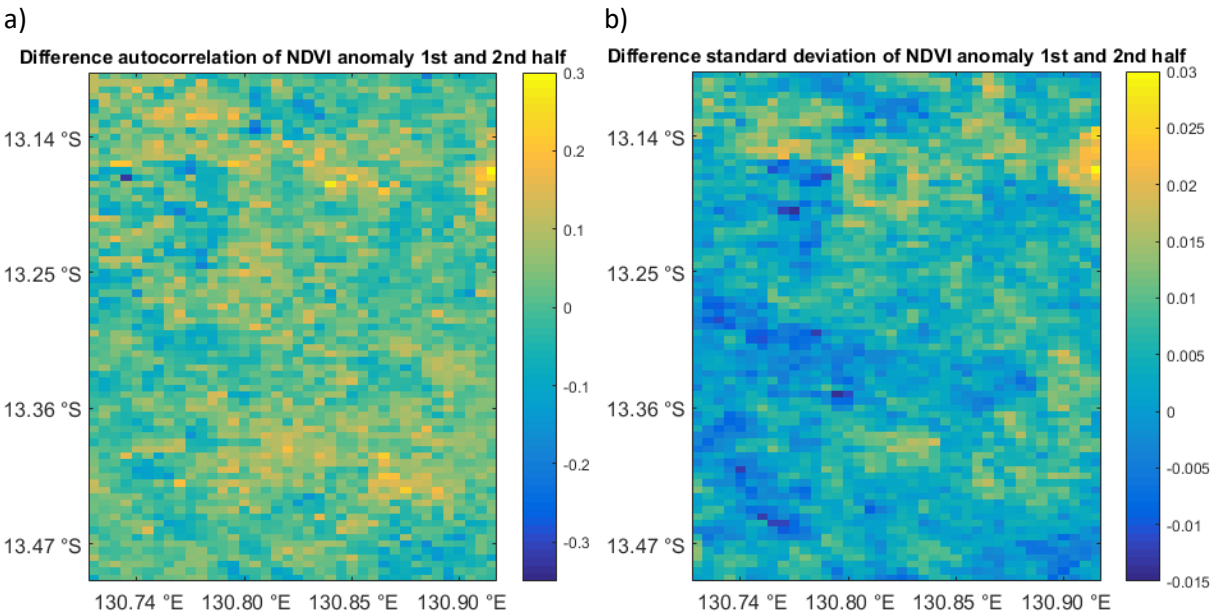

Figure 5.8 (a): Difference between the autocorrelation of the first half (November 2001 – December 2008) and second half (January 2009 – September 2016) of the time series. Positive values correspond to an increase in autocorrelation over time, whereas negative values to a decreasing autocorrelation over time; (b): Difference between the standard deviation of the first half and second half of the time series. Positive values correspond to an increase in standard deviation over time, whereas negative values to a decreasing standard deviation over time.

Plotting the stability change classes (Figure 5.9) indicates that more than half of the study area (53.72%) increases in autocorrelation and standard deviation between the first (2001-2008) and second half (2009-2016) of the time series. 24.77% shows a decreasing autocorrelation trend and an increasing standard deviation, 16.07% reveals a decreasing trend in both indicators and only 5.44% shows a decreasing standard deviation and increasing autocorrelation signal over time.

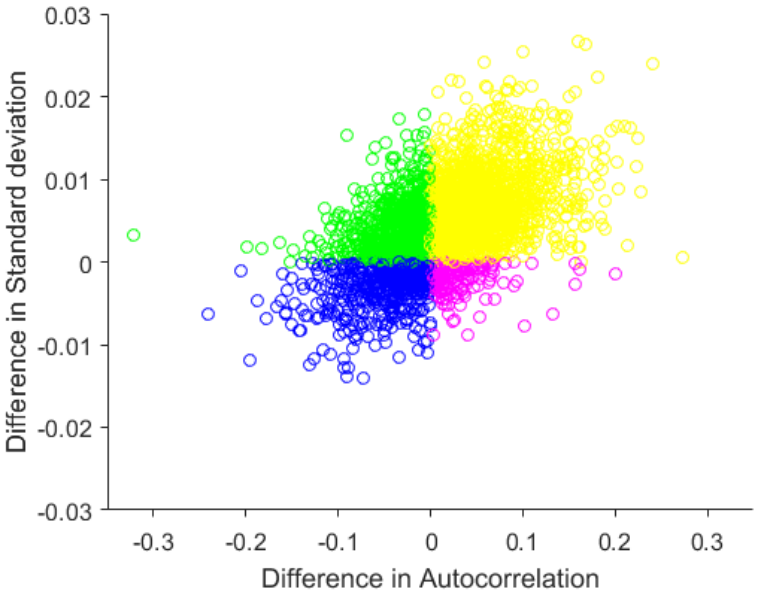

Figure 5.9: Four categories can be made from the combination of the autocorrelation and standard deviation trends between the first (2001-2008) and second (2009-2016) half of the time series. 53.72% of the study area increases in both autocorrelation and standard deviation (yellow), 24.77% decreases in autocorrelation and increases in standard deviation (green), 16.07% decreases for both indicators (blue) and lastly 5.44% decreases in standard deviation and increases in autocorrelation (magenta).

The spatial patterns of the stability change classes (Figure 5.10) display a domination of the increasing trends of both autocorrelation and standard deviation, corresponding to a decreasing vegetation resilience and higher susceptibility to climate anomalies. Decreasing trends of both indicators, so a higher resilience and lower susceptibility of the ecosystem, are mostly visible on the west side of the study area and in the south east corner. Areas with a decrease in autocorrelation and increase in standard deviation are mostly located on the east side of the study area, but show also a fairly scattered pattern. Areas with a decreasing standard deviation and increasing autocorrelation between the two time periods cover the smallest area with a concentration around the 13.32 °S latitude.

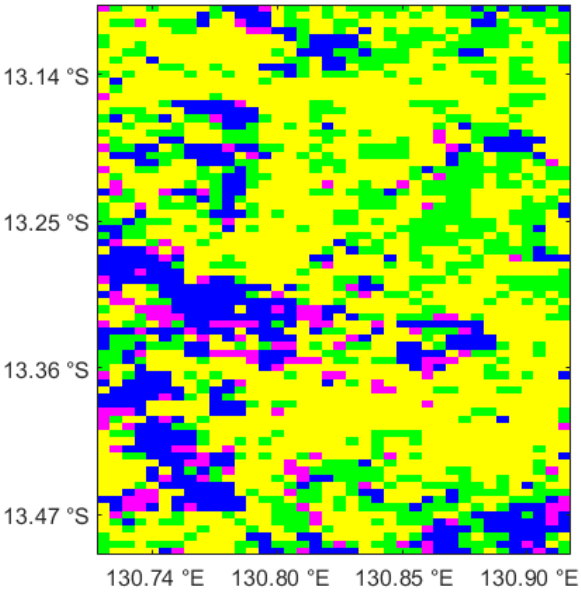

Figure 5.10: Four categories can be made from the combination of the autocorrelation and standard deviation trends between the first (2001-2008) and second (2009-2016) half of the time series. Yellow areas indicate an increase in both metrics, green marks the areas with a decrease in autocorrelation and an increase in standard deviation, blue the areas with a decrease for both metrics, and magenta an increase in autocorrelation and a decrease in standard deviation.

5.3 Linking woody cover and ecosystem's short-term stability

The aim of this thesis research is to gain a deeper understanding on the relationship between woody cover dynamics and the ecosystem's short-term stability. Therefore spatial and temporal patterns of both variables are compared and analysed. Furthermore, the dynamics of fire frequency and bare soil coverage in the area are also looked into in this subsection as possible extra explanatory variables of the ecosystem's short-term stability dynamics.

5.3.1 Spatial patterns

Comparing the spatial patterns of both short-term stability metrics, namely the autocorrelation (Figure 5.5) and standard deviation (Figure 5.6) of the NDVI anomaly signal, and the average DSI (Figure 5.1, a) over the total time span (November 2001 – September 2016) shows some interesting similarities and contrasts. The areas that show a higher DSI value (region A, B and C) correspond to the higher autocorrelation and standard deviation regions. Remarkably, the region around 13.4190 °S, 130.7684 °E which appears to have one of the highest average DSI values, shows lower values for both metrics and goes so against the recently stated hypothesis. A second contrast to be noticed is region D on the east side that has one of the highest autocorrelation values and a high standard deviation, but shows exclusively low to average DSI values. Plotting the DSI against both indicators displays a significant

positive relationship between the DSI and the standard deviation (Figure 5.11, a) with a correlation coefficient of 0.15 and a significant negative relationship between the DSI and the autocorrelation (Figure 5.11, b) with correlation coefficient -0.12.

a) b)

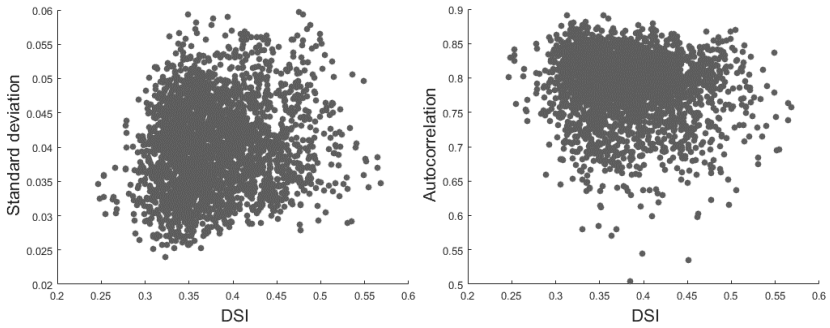

Figure 5.11 (a): There exists a positive relationship between the DSI and the standard deviation with a significant (p<0.05) correlation coefficient of 0.1491 (p = 2.87E-15). The DSI versus the autocorrelation reveals a negative influence on each other with a significant (p: 4.88E-10) correlation coefficient of -0.1178.

Given that the DSI does not completely explain the spatial patterns of the stability metrics, spatial patterns of fire frequency and bare soil coverage are also examined. When observing the fire frequency of the area over the total time series (Figure 5.12, a), it is striking that there exists a large contrast between areas that did not burn the entire time whereas other areas burned up to 16 times in the 15 year time span. The area showing a low fire frequency further coincides with a bare soil coverage above roughly 20% (Figure 5.12, b). The overall mean bare soil coverage for the total study area is 10.39% $\pm$ 5.59%.

a) b)

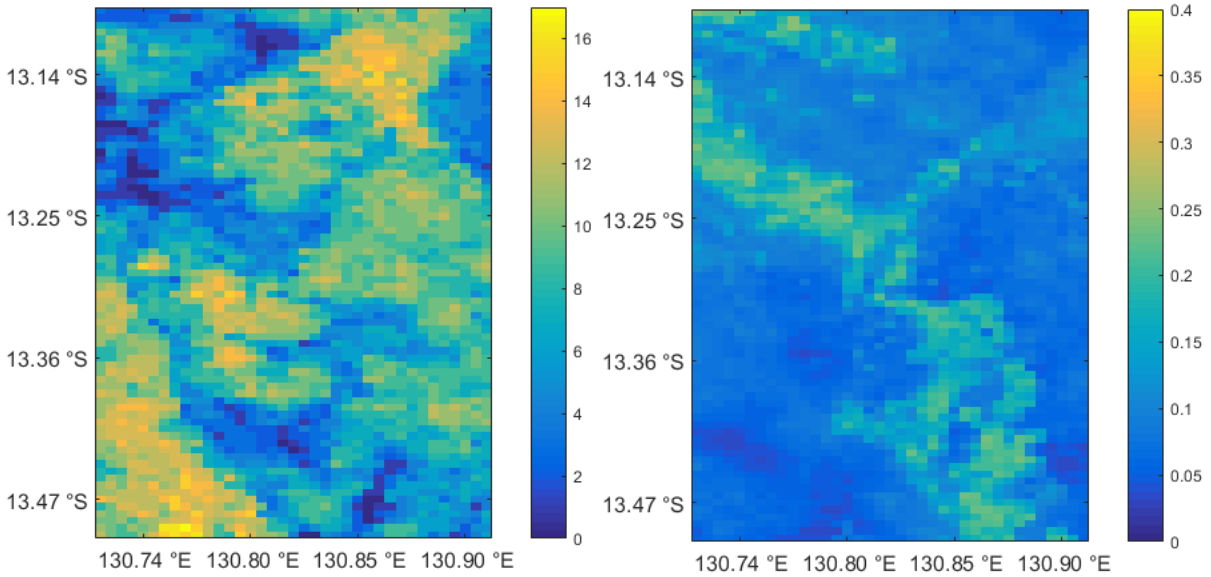

Figure 5.12 (a): The total amount of fire events that took place in the area between 2002 and 2016 ranges between 0 and 16; (b): The average VCF bare soil coverage over the total area from 2002 to 2016 shows higher bare soil coverage at the diagonal from the north west corner to the south east border.

A comparison between the fire frequency from 2002 to 2016 (Figure 5.13) and the short-term stability indicators shows more or less resembling spatial patterns between the three. This is expressed in the significant positive correlation coefficients of 0.45 for the standard deviation and 0.31 for the autocorrelation. Again a higher correlation is at stake for the standard deviation metric than for the autocorrelation.

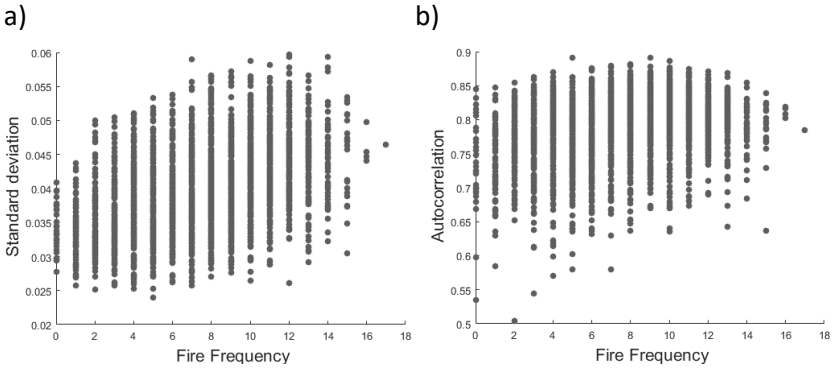

Figure 5.13 (a): Scatterplot of the standard deviation (2001-2016) and the fire frequency from 2002 to 2016 displays a positive relationship between both variables with a significant (p = 8.05E-142) correlation coefficient of 0.4549; (b): The fire frequency from 2002 to 2016 has a positive effect on the autocorrelation (2001-2016) with a significant (p = 6.20E-64) correlation coefficient of 0.3125.

A scatter plot between the VCF average bare soil cover and the two short-term stability indicators (Figure 5.14) illustrates two times a negative relation. The correlation coefficient for the relationship between the average bare soil coverage and the standard deviation is -0.45, and for the relationship with the autocorrelation it returns a correlation coefficient of -0.32. Comparing these correlation coefficients with those of the fire frequency and the stability indicators reveals almost completely contrasting results. Whereas the fire frequency had a positive relationship with the standard deviation of 0.45, the VCF bare soil cover has a negative relationship of -0.45. Similar for the autocorrelation, the absolute values of the relationship versus the fire frequency and versus the bare soil coverage are almost alike, but differ in sign.

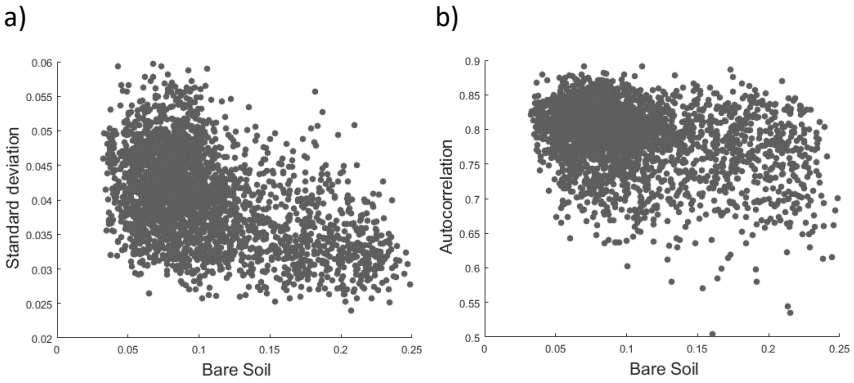

Figure 5.14 (a): The average bare soil (2002-2015) shows a negative relationship with the standard deviation (2001-2016) with a significant (p = 2.54E-140) correlation coefficient of -0.4527; (b) The average bare soil cover (2002-2015) has a negative impact on the autocorrelation (2001-2016), as the significant (p = 1.38E-66) correlation coefficient is here -0.3188.

Now that the potential driving factors of the ecosystem's short-term stability have been characterised, a multivariate linear regression model is defined for each of the stability indicators. Figure 5.15 displays the distribution of all the significant ($p<0.05$) estimates and the overall mean estimate of every predictor variable on the autocorrelation. From this it can be observed that both the DSI and bare soil coverage have a negative impact on the autocorrelation whereas the fire frequency has a positive effect on the autocorrelation. From an ecological perspective it can thus be said that the DSI and bare soil make the ecosystem more resilient as they fasten the recovery speed of the vegetation whereas the fire frequency increases the recovery time of the vegetation and so makes it less resilient. For this model the VIF values ranged between 6.69 and 377.92, marking highly correlated predictor variables.

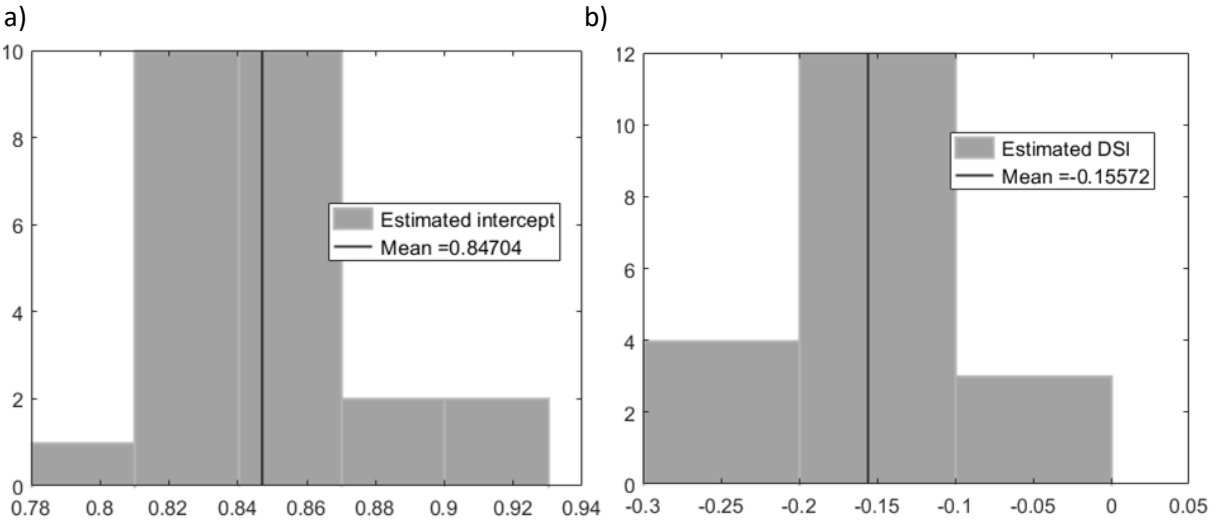

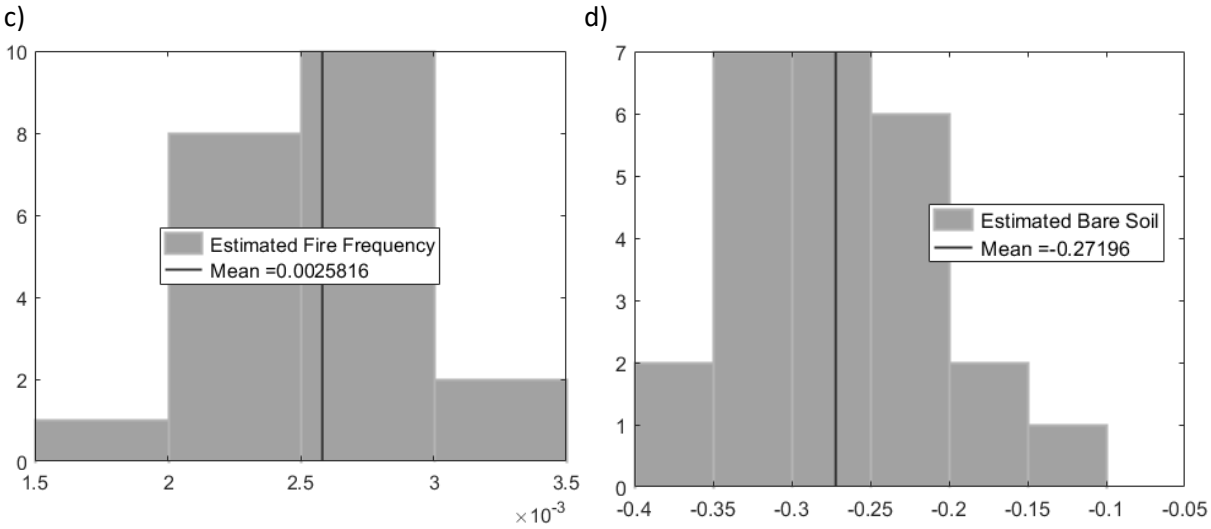

Figure 5.15 (a): Distribution of the significant (p<0.05) estimated intercepts for the autocorrelation and the overall mean value; (b): Distribution of the significant estimated DSI predictor variables and its overall mean value; (c): Distribution of the significant estimated fire frequency predictor variables and its overall mean value; (d): Distribution of the significant estimated bare soil predictor variables and its overall mean value.

In the case of the standard deviation, the distributions of the DSI and fire frequency illustrate a positive effect on the standard deviation whereas only bare soil shows to have a decreasing effect on the standard deviation. So, the DSI and fire frequency increase the susceptiblity of the vegetation whereas the bare soil coverage strengthens the ecosystem and makes it more insensitive to changes or disturbances. The distributions of all the estimates of the predictor variables are presented in Figure 5.16. Table 5.1 gives for every predictor variable the percentage of repeats with a significant (p<0.05) estimated value and Figure 5.17 illustrates the distribution of the Root Mean Square Errors (RMSE) of both models and their mean value. Also this time the VIF values of the predictor variables indicate a high correlation between the predictor variables as they range between 5.85 and 113.64.

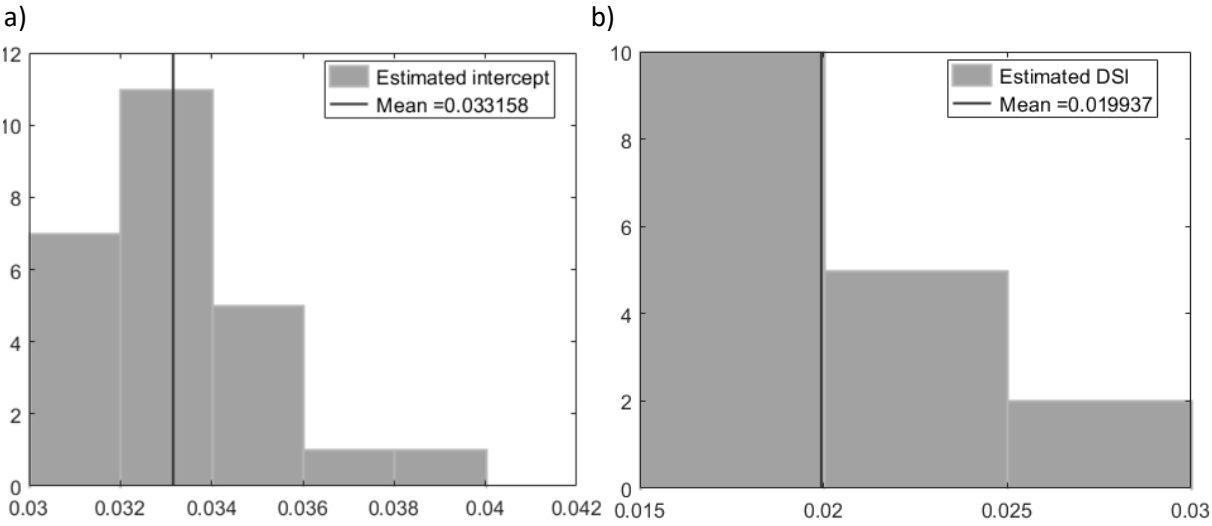

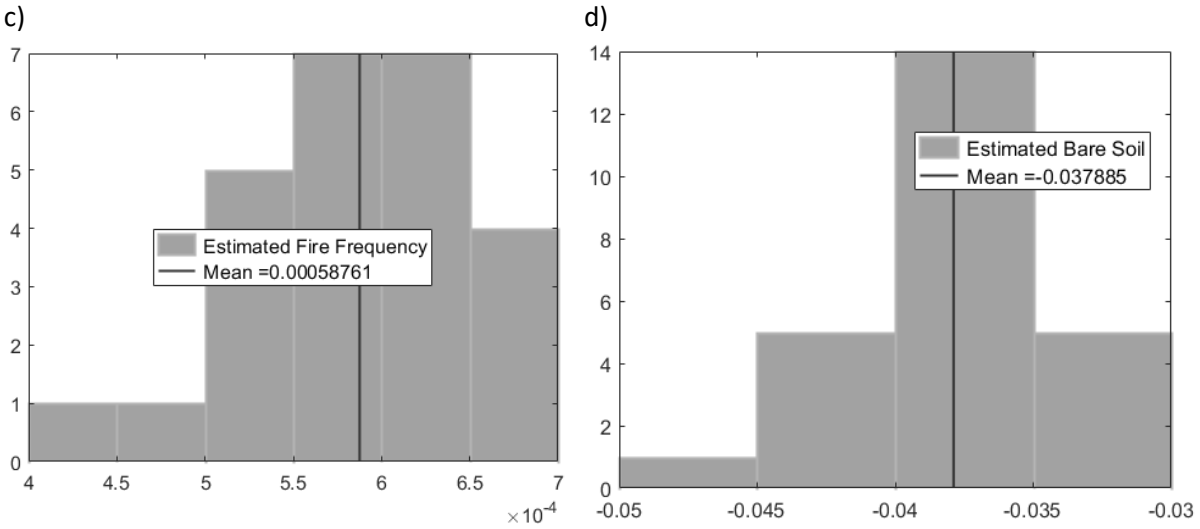

Figure 5.16 (a): Distribution of the significant (p<0.05) estimated intercepts for the standard deviation and the overall mean value; (b): Distribution of the significant estimated DSI predictor variables and its overall mean value; (c): Distribution of the significant estimated fire frequency predictor variables and its overall mean value; (d): Distribution of the significant estimated bare soil predictor variables and its overall mean value.

Table 5.1: For every variable of the autocorrelation and standard deviation models the percentage of repeats with a significant p value (p<0.05) are represented.

	Percentage significant	
	Autocorrelation	*Standard deviation*
Estimated intercept	100%	100%
Estimated DSI	76%	68%
Estimated Fire frequency	84%	100%
Estimated Bare soil	100%	100%

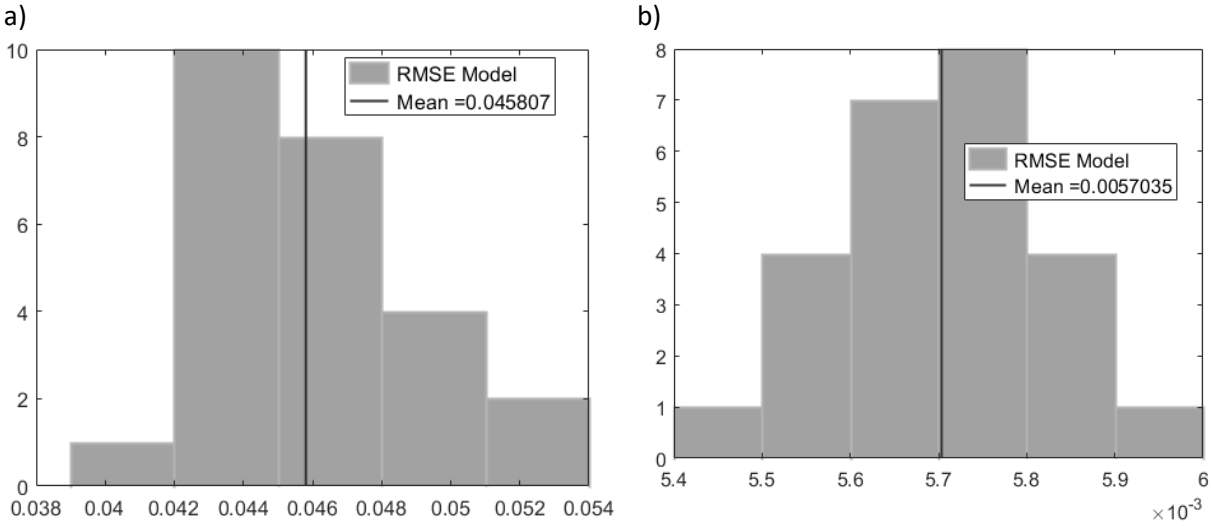

Figure 5.17 (a): Histogram of the RMSE's for the 25 repeats of the multivariate linear regression model with the autocorrelation as response variable; (b) Histogram with the RMSE's for the 25 repeats of the multivariate linear regression model of the standard deviation.

5.3.2 Temporal patterns

As clear differences are noticed between the stability metrics over the first and second half of the time series (Figure 5.8), a closer look was also taken into the temporal trends of the predictor variables. The changes in the DSI (Figure 5.18, a) vary from increments up to 0.0068 to decreases up to -0.045, with both extremes located in the north west. The area with maximal positive change is surrounded by several patches that also show increases whereas the north east corner is characterized by decreasing DSI trends over time. Woody cover in the southern areas changes in smaller proportions and shows a more scattered pattern. The VCF bare soil coverage (Figure 5.18, b) shows over the total extent a higher percentage of pixels where the bare soil coverage increased over time. Though, a larger patch of decreasing bare soil trends is visible on the eastern border of the study area. Figure 5.18, c reveals a noticeable higher amount of fire events (3 to 7) on the east side of the study area for the second time period. Two spots on the left at the 13.16 °S and the 13.36 °S latitude also show more fire events between 2009 and 2016 than between 2002 and 2008. Patches were less fire events found place in the second time period are more dispersed over the total study area.

a) b)

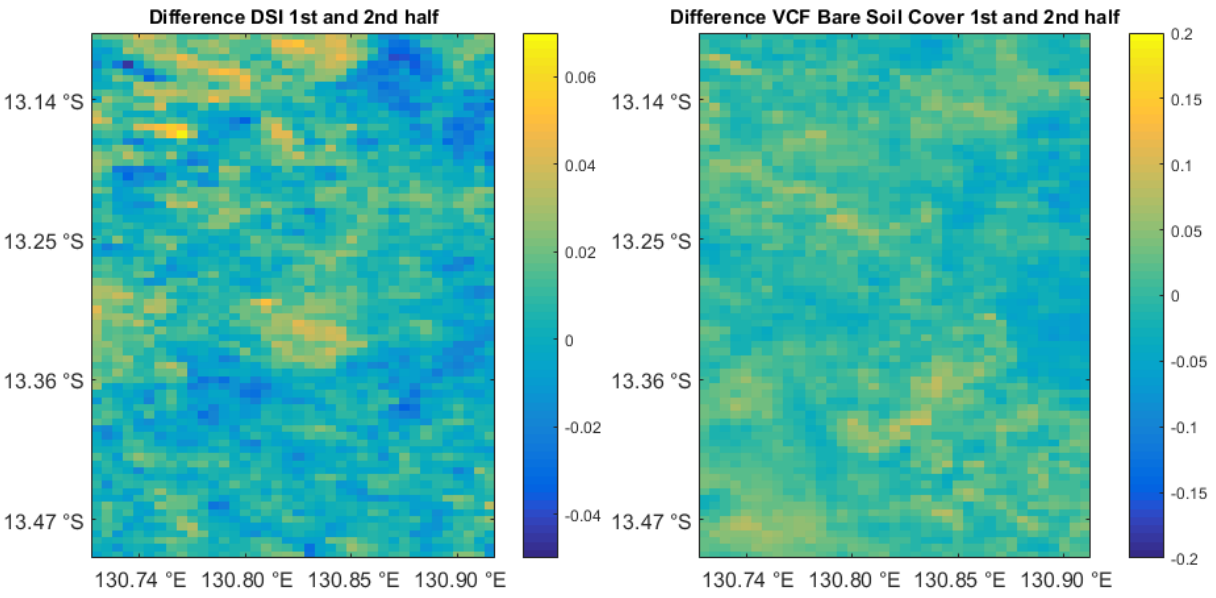

c)

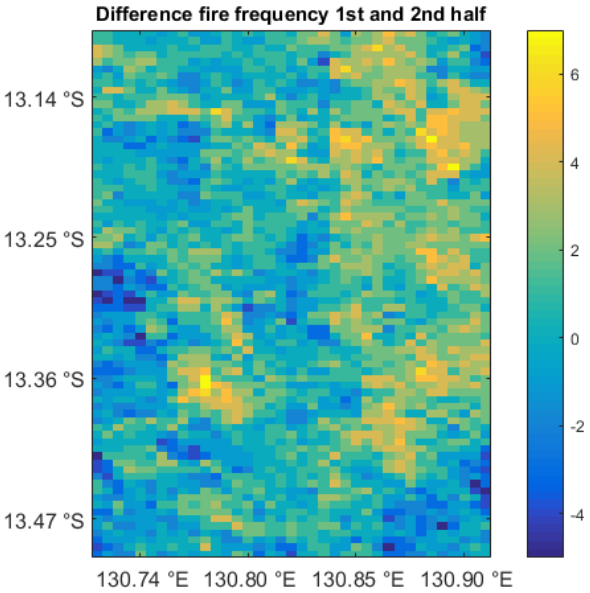

Figure 5.18 (a): The difference in DSI displays the woody cover trend between two time intervals (2001-2008 and 2009-2016) for every pixel. Positive values indicate an increase in woody cover between the two time periods whereas negative values represent a decreasing woody cover; (b): The difference in VCF bare soil coverage reveals the increasing or decreasing trend of bare soil coverage between the time periods 2002-2008 and 2009-2015 for every pixel; (c): The difference in fire frequency displays the increasing or decreasing trend in amount of fire events between the two time periods (2002-2008 and 2009-2016) for every pixel.

Putting all these variables in a multinomial logistic regression allows to get an idea how the predictor variables have an influence on the temporal trends of the autocorrelation and standard deviation. The estimates express the effects of the predictor variables on the log odds of being in one category versus the reference category. It must be noted though that in this situation (Table 5.2) conclusions have to be made with caution as the obtained results have changing reliabilities. For some variables even no conclusions can be made as there were no replications with a p value below the significance threshold of 0.05. For the DSI it can stated with a reliability of 36% that the estimated coefficient of -4.6851 indicates that the probability of being in the first category (increasing autocorrelation and standard deviation) compared to the probability of being in the third category (decreasing autocorrelation and standard deviation) decreases exp(-4.6851) times for each unit increase in DSI, given all else equal. When comparing the second category (decreasing autocorrelation and increasing standard deviation) and the third category, again a higher probability of being in the third category is at stake. The intercept on the other hand has in both situations, so first category versus third category and second category versus third category, a higher probability with each unit increase for the non-reference category. Comparing the response variables mutually, there exists a lot of variation in reliability. The estimated coefficients of fire frequency and bare soil only receive a maximal reliability of 8%.

Table 5.2: Multinomial logistic regression analysis with the DSI, fire frequency and bare soil coverage as predictor variables and the categories of combined autocorrelation and standard deviation trends as response variables. A+ corresponds to an increasing autocorrelation trend between the first (2001-2008) and second (2009-2016) time period, A- to a decreasing autocorrelation trend. SD+ expresses an increasing standard deviation and SD- a decreasing standard deviation over time. The percentage of repeats with a significant p value ($p<0.05$) according to the t-statistic is first presented for every predictor variable and the intercept, followed by the mean estimate, the standard error (SE) and the t-statistic. Positive estimates correspond to a higher probability of being in the category of the numerator whereas negative estimates correspond to a higher probability of being in the category of the denominator.

		Intercept	***DSI***	***Fire Frequency***	***Bare Soil***
$\frac{\mathbf{A+, SD+}}{\mathbf{A-, SD-}}$	*Percentage*	72%	36%	8%	0%
	Estimate	3.5083	-4.6851	-0.2000	
	SE	1.1051	1.9743	0.0792	
	t-Statistic	3.3028	-2.3502	-2.5281	
$\frac{\mathbf{A-, SD+}}{\mathbf{A-, SD-}}$	*Percentage*	64%	60%	8%	0%
	Estimate	3.9246	-5.8653	-0.1844	
	SE	1.0913	2.0648	0.0836	
	t-Statistic	3.6902	-2.8165	-2.2095	
$\frac{\mathbf{A+, SD-}}{\mathbf{A-, SD-}}$	*Percentage*	0%	0%	4%	8%
	Estimate			-0.1814	-14.8739
	SE			0.0833	5.9820
	t-Statistic			-2.1782	-2.4870

6 DISCUSSION

6.1 Woody cover estimation

This study assesses the woody cover dynamics in Litchfield National Park using the Dry Season Index (DSI). With the ongoing climate change, future prospects of this national park, situated in the Australian tropical savannas, are to a large extent depending on the relationship between woody cover and the ecosystem's short-term stability (Hughes 2003; IPCC 2014; Brandt et al. 2016). This study aims to provide insight in this relationship.

The DSI is introduced by Brandt et al. (2016) as an improved proxy for woody cover by including vegetation metrics covering various stages of the growing season cycle. Choosing a high temporal resolution for the assessment of woody cover is considered to be a valuable asset in semi-arid to arid regions where vegetation is marked by a phenological cycle that is driven by the interaction of a dry and wet season (Brandt et al. 2016). In the area that is subject of this study, the climate is known to have a highly seasonal character with summer monsoons that involve high inter-annual variabilities in rainfall seasonality and intensity, and high air temperatures (Bowman & Prior 2005). As a consequence, the availability of relevant data that are not affected by clouds, varies. In particular for the wet season, 66.25% to 87.50% of the data in this study were labelled as low quality data. As the DSI takes both dry season and wet season into account, smoothening and interpolation was needed to reduce the influence of these missing and low quality data.

6.1.1 Spatial patterns

Tropical savannas thrive by the constant interaction between disturbance events like fires and cyclones and its consecutive recovery. Within such dynamic ecosystem, regional variations in woody cover can occur. According to the average DSI over the total study area, there are two regions in Litchfield National Park where woody cover is roughly a DSI of 0.10 to 0.20 higher than the overall mean DSI of 0.3794. The environmental elements summed below, are identified as major influential factors to this regional variation in woody cover. Fire is a first important driver in woody cover dynamics. Although intense fires have the power to decimate patches of trees and growing seedlings, simultaneously a lot of savanna tree species feature physical characteristics adapted to the frequent occurrence of fire. In Litchfield National Park eucalypts dominate the upper storey and are characterized by a specific bark layer that protects them against fire events (Lawes et al. 2011). A second important explanatory factor of the regional variation in woody cover is the rainfall gradient, increasing from the south to the north of the park (Lawes et al. 2011). Thirdly, variability in soil type and rain water redistribution patterns

have also been put forth as contributing factors (Brandt et al. 2016). Moreover, in a study on the impact of feral buffalo on woody cover growth in Kakadu National Park, 170 km east of Litchfield National Park, Bowman et al. (2008) concluded that buffalos had a minor influence on the woody cover dynamics. For eucalypt savannas, the presence of buffalos, be it in low densities, was found to yield the highest canopy cover increases. A last explanatory factor was found from mapping the digital elevation model from NASA's Shuttle Radar Topography Mission (SRTM) imagery with a spatial resolution of 90 m (Figure 6.1) (Tom et al. 2008). The spatial patterns of this elevation model rise the assumption that the higher woody cover areas are located on areas were topography is less complex and so more gentle. Furthermore, it is also possible that there exist interactions between some of these factors, for example that buffalos are more present at certain altitudes or that they mostly graze at gentle sloping areas.

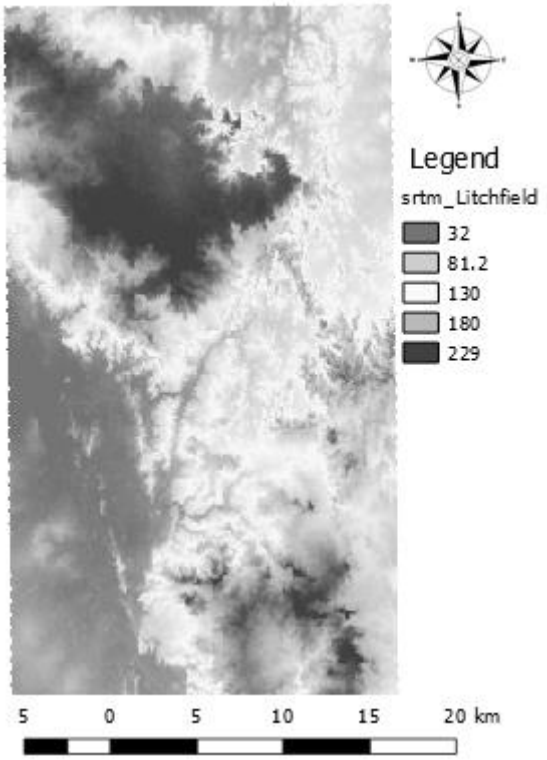

Figure 6.1: Digital elevation model from NASA's SRTM imagery of the study area in Litchfield National Park, ranging from 32 metres to 229 metres.

6.1.2 Comparison with VCF tree cover product

Comparing the average DSI and average VCF tree cover product over the total extent of the study area in Litchfield National Park reveals highly resembling spatial patterns. Both variables assess the woody cover of the study area but are expressed in a different way. The VCF tree cover product, as part of a surface cover product, assesses the percentage of tree cover in the area. The DSI is not expressed as a

cover percentage, but as a unitless index related to woody cover (i.e. the DSI increases when woody cover rises). Apart from the different ways in expression, there is also a distinction to be noticed in what they exactly measure. While the DSI is developed to be a proxy for woody cover in semi-arid regions (Brandt et al. 2016), the VCF tree cover product only detects tree canopies above 5 metres and does not take woody canopies of small trees, shrubs and bushes into account (Hansen et al. 2002; Townshend et al. 2011). This causes a fair underestimation of the total woody cover present in the Litchfield National Park when solely relying on the VCF tree cover product. Similar observations were found in the study of Brandt et al. (2016) for their study sites in Senegal and Mali. The VCF tree cover product is hence developed to detect deforestations or increments of tree canopies in (dense) forests. Savannas on the other hand are typically characterized having a continuous layer of grasses and herbs, interspersed with patches of trees and shrubs, and are therefore not at all dense. This discontinuous layer is however considered very important to savanna ecosystems as they define for the largest part the productivity of this ecosystem (Brandt et al. 2016).

The inter-annual variability of the VCF tree cover and DSI woody cover estimates exposes a higher susceptibility to changes of the VCF tree cover product compared to the DSI. The ratios of the standard deviations over the overall mean value have not only a wider range but reach also a higher maximum for the VCF tree cover. This higher variability can largely be attributed to the inter-annual smoothening process that was performed on the DSI calculations and not on the VCF tree cover product. Going over all the years separately, DSI values fluctuate little around the average value and spatial patterns do not change that much, whereas VCF tree cover percentages fluctuate heavily and reveal changing spatial patterns almost every year. Additional explanations for this fickle behaviour can be the difference in temporal resolution between both variables and possible confusion with a dense mid-storey of lower lying shrubs and palms (MODIS Land Team 2016). A lower temporal resolution (16 days against 8 days) causes a higher uncertainty which in this situation results in a higher variability of the end product.

6.1.3 Temporal patterns

Over the total study area only 25.26% of the pixels show a significant trend in woody cover (DSI) over the total time series (2002-2016), varying from a loss of woody cover (5.54%) up to a DSI of -0.0052 to an increasing DSI (19.72%) of 0.0087. Increases in foliage density may be attributed to a combination of driving factors that steer this tropical ecosystem. Firstly, variability in climate, as a consequence of climate change and of the El Niño Southern Oscillation periodical variation, causes high inter-annual variability in rainfall. However, an overall increasing trend in rainfall across Australia has been witnessed over the past century. Across northern Australia however, this tendency has been more

outspoken as of the 1970's period (Figure 6.2, a) (Bowman et al. 2001; Hughes 2003). This higher rainfall is the result of an increment in the number of rain days and heavy rainfall events. Besides an increase in rainfall, annual temperatures have also been found to increase since the past century (Figure 6.2, b), although less outspoken than the rainfall increase (Hughes 2003).

Secondly, changes in fire regime with cessation of the Aboriginal landscape burning practices and introduction of controlled burning programs (Bowman et al. 2001) are put forth as one of the primary causes (Lehmann et al. 2009; Laurance et al. 2011). Fires can have a destructive force, or in cases of low intensity destroy the herbaceous layer which allows a quick regrowth or further expansion of tree seedlings, fuelled by the extra nutrients of the ashes. Murphy et al. (2014) however warn that high fire frequencies or intense fires are able to destroy all vegetation, including upper woody cover layers, and hereby reverse the woody thickening trends. An additional danger that can contribute to this reverse in woody cover is the alarming spread of invasive weeds and grasses like Gamba grass (*Andropogon gayanus*). Besides transforming fire regimes, they are also able to alter other fundamental ecosystem attributes such as carbon storage and nitrogen cycling (Laurance et al. 2011).

Furthermore, the overall rising CO_2 level has also been listed as a contributing factor of vegetation growth in water limited environments (Donohue et al. 2009). Elevated CO_2 levels namely reduce the stomatal conductance and hereby enhance the water use efficiency of plant species (Hughes 2003), mitigating survival in drier conditions. Increases in CO_2 level can also be linked with fire as they increase the fuel load through enhancement of the primary productivity (Donohue et al. 2009). The magnitude of this increasing plant growth phenomenon, also referred to as 'CO_2 fertilization effect', is however strongly dependent on the availability of water and nutrients like nitrogen and phosphorus, and causes therefore some uncertainty (Hughes 2003).

Given that increases in woody cover (DSI) in the study area are (i) occurring more frequently (19.72% versus 5.54%) and (ii) larger in magnitude than losses of woody cover (up to 2.29% against 1.37%), are an indication that woody thickening is taking place in Litchfield National Park. The overall results of a slight increase in woody cover correspond to the observations of Lehman et al. (2009) in their study on Kakadu National Park and of Murphy et al. (2014) studying woody biomass dynamics in Kakadu, Nitmiluk and Litchfield National Park, in which both only remark little net changes in woody biomass.

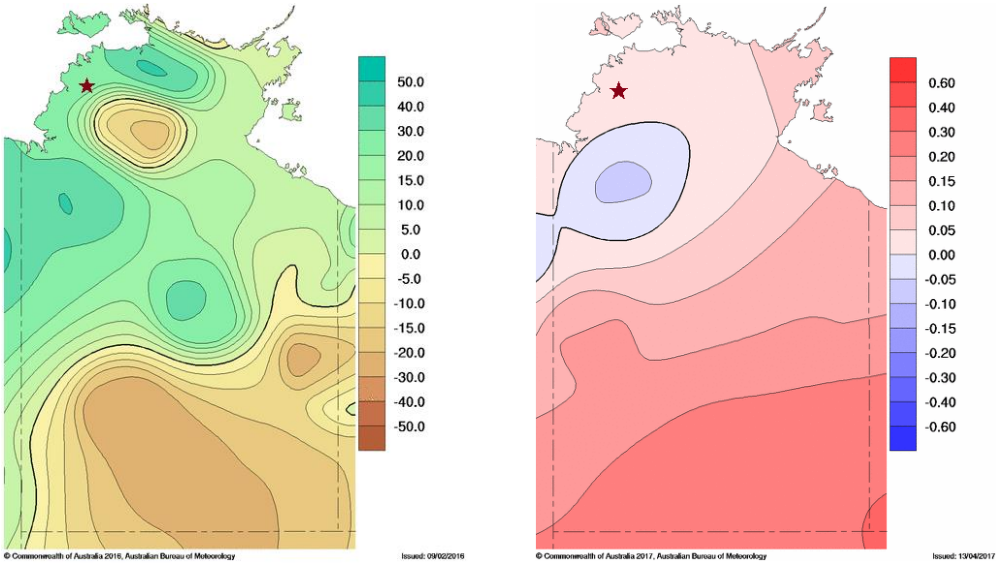

Figure 6.2 (a): Trend in annual rainfall of the Northern Territory between 1970 and 2015, expressed in mm per 10 years. The study site, situated in Litchfield National Park, is marked by a red star; (b*): Trend in mean temperature of the Northern Territory between 1970 and 2016, expressed in °C per 10 years. The study site is again marked by a red star*.

6.2 Impact of woody cover on ecosystem's short-term stability

6.2.1 Spatial patterns

In order to characterize the short-term stability of the Australian tropical savanna ecosystem, time series of the DSI and of the autocorrelation and standard deviation of the NDVI anomaly were investigated on a spatial and temporal level across our study area in Litchfield National Park. As stability may be driven by other variables besides the woody cover (DSI) , both fire frequency and bare soil coverage were added as extra explanatory factors. From the multivariate linear regression model and the mutual correlation plots (Figure 5.11), a positive relationship between woody cover (DSI) and the variance (standard deviation of the NDVI anomaly) of the ecosystem can be observed. So this means that an increase in woody cover enlarges the variance of the ecosystem and makes it therefore more susceptible to changes or disturbances. Woody cover and autocorrelation on the other hand have a negative relationship, meaning that an increment of the woody cover results in a more resilient ecosystem as it fastens the recovery speed. Fire frequency has a positive relationship with both standard deviation and autocorrelation (Figure 5.13), indicating that the susceptibility of the ecosystem towards changing events increases and that the recovery speed decreases after such events, corresponding to a declining resilience. Lastly, bare soil coverage has the opposite effect of fire frequency as it decreases the variance, making the ecosystem more insensitive to changes, and speeds up the recovery after disturbances or changes, making it more resilient (Figure 5.14).

6.2.2 Uncertainties about the explanatory factors

When analysing the woody cover estimations, it has to be taken into account that the applied methodology of the DSI, developed by Brandt et al. (2016), is based on several assumptions and involves choices which may introduce uncertainties. Firstly, the DSI assesses woody cover through calculation of the greenness intensity of the foliage of woody plants, assuming that woody biomass only consists of one layer. Secondly, the assumption is made that in a time period of 15 years (2002-2016) meaningful and linear trends may be observed. Short-term variations in foliage density are however present and are the effect of climatic and anthropogenic factors (Broich et al. 2014), including short-term variability in rainfall due to the influence of the El Niño Southern Oscillation (Nicholls et al. 1997), grazing pressure and burning practices. As a consequence, they create uncertainties in the identification of longer-term woody cover trends (Brandt et al. 2016). Thirdly, uncertainties are also introduced through the fact that fluctuations in dry season NDVI, caused by inter-annual variabilities in growth conditions during the wet season, are only attenuated when a significant ($p<0.05$) relationship between the wet season maximum NDVI and the following mean dry season NDVI was present. In case no significant relationship existed, no correction factor was applied, leading to uncertainties in these regions.

In addition, there always exists some correlation between the explanatory factors. If this correlation is close to one (i.e. minimal), the impact is negligible but if factors are highly correlated, it reduces the reliability of the entire model. This statistical phenomenon of multicollinearity complicates the interpretation of the final model as it increases the standard errors of the coefficients and can likewise result into insignificant variables when they should actually be significant (Martz 2013). To assess how much the standard deviation of an estimated regression coefficient increases if predictors are correlated, the variance inflation factor (VIF) can be calculated. The statistics of this study show that the predictor variables are faced with multicollinearity, which obstructs to some extent the final interpretation of the effects each factor has on the eventual short-term stability metrics. A solution to deal with multicollinearity is to remove highly correlated predictors from the model one by one. An alternative method is to use partial least squares regression or principal components analysis to reduce the number of predictors to a smaller set of uncorrelated components (Martz 2013).

6.2.3 Temporal changes

Analysing the combined changes of the vegetation variance (standard deviation) and resilience (autocorrelation at lag-1) between the first half of the time series (November 2001 – December 2008)

and the second half (January 2009 – December 2016), reveals that more than half of the study area in Litchfield National Park has gotten less resilient and more sensitive to fluctuations in NDVI anomaly. Combining these results with the changes in woody cover (DSI), fire frequency and bare soil via the multinomial logistic regression allows to make predictions on the impact of a temporal change of any of these factors on the variance and resilience. From these analyses many relationships were not significant which do not allow to make solid statements. Nevertheless, it can be concluded that an increasing woody cover over time most likely results in a more resilient ecosystem as the autocorrelation decreases, and in an ecosystem less susceptible to changes or disturbances as the standard deviation decreases as well. With a maximal significance percentage of 8% the same can be said about the fire frequency, namely that an increasing fire frequency most likely would lead to a more resilient and less susceptible ecosystem. These results however do not have knowledge on the intensity of these fire events. For bare soil it can only be stated with a significance percentage of 8% that an increase in bare soil would rather lead to a more resilient ecosystem that is more insensitive to changes than to a less resilient ecosystem but still more insensitive to fluctuations caused by disturbances or changes.

Comparing the results at the temporal and spatial level reveals interesting contrasts. Whereas the increase in woody cover corresponded to an increment of the ecosystem variance at the spatial level, it showed a negative relationship at the temporal level. These differing results can possibly be attributed to a lower percentage of significant relationships which creates a higher uncertainty. Fire frequency displays completely contrasting results between the spatial and temporal level. Here of course, the reliability of the temporal change results is smaller as there were only 8% of the relationships significant against 84% and 100% for the spatial variability. Bare soil on the other hand showed as only explanatory factor similar results at both the spatial and temporal scale. Here again however, the significance percentage is not favourable and does not allow yet to make firm conclusions.

Since there is a general consent about the woody thickening of the Australian savannas given the current influences of climate change (Bowman et al. 2001; Donohue et al. 2009; Lehmann et al. 2009; Ahlström et al. 2015), it can be predicted that this increase in woody cover most likely would lead to a more resilient ecosystem. The overall results of the variance cannot straightforwardly be interpreted and therefore need further observation.

6.2.4 Proposed improvements

As this study is faced with some uncertainties regarding the assessment of the woody cover via the DSI and regarding the mutual correlation of woody cover, fire frequency and bare soil coverage, further improvements can be made to better assess the impact of woody cover dynamics on the variance and resilience of this Australian tropical savanna ecosystem. This dynamic ecosystem is driven by multiple climatic, biological and anthropogenic factors, causing a number of possible explanatory factors that might be involved in this woody cover short-term stability story. Already pointed out as an important driver of this ecosystem, climate variability might be a crucial factor that can further optimize this relationship between woody cover and the ecosystem's short-term stability. This variability is to a large extent caused by the variability in rainfall which defines if there is an excess or deficit of water every year, and so controls the productivity of the ecosystem. According to Gallant et al. (2013) there is a trend since 1911 towards less frequent, shorter and less severe droughts in northern Australia. Monitoring the inter-annual variability in rainfall can therefore tell if drought was a limiting factor at any moment in time or not. At the spatial extent it is likely though that as this is a relatively detailed study on Litchfield National Park, this gives only minor variations. An index that provides this specific information is for example the Standardized Precipitation-Evapotranspiration Index (SPEI). A short analysis on our study area with the global SPEIbase dataset, developed using the Global 0.5° gridded Climate Research Unit (CRU) TS3 monthly precipitation and mean temperature data (Vicente-Serrano et al. 2010), implies with an average SPEI value of -0.0748 that there is a deficit of water in the period from 2002 to 2008. From 2009 to 2016 on the other hand the average SPEI has a value of 0.2951 which indicates an excess of water. Other factors that might have an impact on the relationship between woody cover and the ecosystem's variance and resilience, and have to be further looked into are the topography and the ground water level (Liu et al. 2009).

7 CONCLUSION

Monitoring the woody cover dynamics via satellite observations of Litchfield National Park, a tropical savanna ecosystem in northern Australia, reveals an overall slight positive growth of the woody biomass from 2002 to 2016. Several factors might be at the base of this increase, including climate variability, a changing fire regime and a rising CO_2 level. Linking this increase of woody cover with the impact on the ecosystem's short-term stability, shows that an increment of woody cover most likely results in a more resilient ecosystem. A growth in woody cover resulted moreover in an increase of the ecosystem's variance at the spatial level but was countered with a decreasing variance at the temporal level. Exploring moreover the spatial impacts of an increase in fire frequency on the stability of the ecosystem point towards a less resilient and more susceptible ecosystem. These results however could also not be confirmed at the temporal level. Increases in bare soil coverage on the contrary lead again to a more resilient ecosystem with a low variance. The explanatory factors are however faced with multicollinearity, which complicates an unbiased vision on each factor separately, and therefore results from this study require to be addressed with caution.

8 REFERENCES

Accatino, F. et al., 2010. Tree-grass co-existence in savanna: Interactions of rain and fire. *Journal of Theoretical Biology*, 267(2), pp.235–242.

Ahlström, A. et al., 2015. The dominant role of semi-arid ecosystems in the trend and variability of the land CO2 sink. *Journal of Geophysical Research: Space Physics*, 348(6237), pp.4503–4518.

Asner, G.P. et al., 2009. Large-scale impacts of herbivores on the structural diversity of African savannas. *Proceedings of the National Academy of Sciences of the United States of America*, 106(12), pp.4947–4952.

Australian Bureau of Meteorology, 2007a. Australian Climate Averages - Decadal and multi decadal Rainfall maps. *Australian Government Bureau of Meteorology*. Available at: http://www.bom.gov.au/jsp/ncc/climate_averages/decadal-rainfall/index.jsp?maptype=1&period=9605&product=totals#maps [Accessed January 10, 2017].

Australian Bureau of Meteorology, 2007b. Australian Climate Averages - Decadal and multi decadal temperature maps. *Australian Government Bureau of Meteorology*. Available at: http://www.bom.gov.au/jsp/ncc/climate_averages/decadal-temperature/index.jsp?maptype=1&period=9605&product=min#maps [Accessed January 10, 2017].

Beringer, J. et al., 2015. Fire in Australian savannas: From leaf to landscape. *Global Change Biology*, 21(1), pp.62–81.

Beringer, J. et al., 2011. Patterns and processes of carbon, water and energy cycles across northern Australian landscapes: From point to region. *Agricultural and Forest Meteorology*, 151(11), pp.1409–1416.

Beringer, J. et al., 2007. Savanna fires and their impact on net ecosystem productivity in North Australia. *Global Change Biology*, 13(5), pp.990–1004.

Boland, D.J. et al., 2006. *Forest Trees of Australia*. DJ Boland, MIH Brooker, GM Chippendale, N Hall, BPM Hyland, RD Johnston, DA Kleinig, MW McDonald, ed., CSIRO Publishing.

Boschetti, L. et al., 2013. MODIS Collection 5 Burned Area Product MCD45. *User Guide*, pp.1–12.

Boundless, 2016. Ecosystem Dynamics. *Boundless: Biology*. Available at: https://www.boundless.com/biology/textbooks/boundless-biology-textbook/ecosystems-46/ecology-of-ecosystems-256/ecosystem-dynamics-947-12207/ [Accessed October 9, 2016].

Bowman, D.M.J.S. et al., 2008. Do feral buffalo (Bubalus bubalis) explain the increase of woody cover in savannas of Kakadu National Park, Australia? *Journal of Biogeography*, 35(11), pp.1976–1988.

Bowman, D.M.J.S. & Prior, L.D., 2005. Why do evergreen trees dominate the Australian seasonal tropics? *Australian Journal of Botany*, 53(5), pp.379–399.

Bowman, D.M.J.S. et al., 2001. Forest expansion and grassland contraction within a Eucalyptus savanna matrix between 1941 and 1994 at Litchfield National Park in the Australian monsoon tropics. *Global Ecology and Biogeography*, 10, pp.535–548.

Brandt, M. et al., 2016. Assessing woody vegetation trends in Sahelian drylands using MODIS based seasonal metrics. *Remote Sensing of Environment*, 183, pp.215–225.

Brandt, M. et al., 2016. Woody plant cover estimation in drylands from Earth Observation based seasonal metrics. *Remote Sensing of Environment*, 172, pp.28–38.

Bristow, M. et al., 2016. Quantifying the relative importance of greenhouse gas emissions from current and future savanna land conversions across north Australia. *Biogeosciences Discussions*, p.47.

Brocklehurst, P., 2008. Ecosystem Regionalisation in the Northern Territory Of Australia: A Conceptual Approach. *Technical report*, 24(21).

Broich, M. et al., 2014. Land surface phenological response to decadal climate variability across Australia using satellite remote sensing. *Biogeosciences*, 11(18), pp.5181–5198.

Browning, D.M. et al., 2008. Woody plants in grasslands: Post-encroachment stand dynamics. *Ecological Applications*, 18(4), pp.928–944.

Carreiras, J.M.B. et al., 2006. Estimation of tree canopy cover in evergreen oak woodlands using remote sensing. *Forest Ecology and Management*, 223(1–3), pp.45–53.

Chen, X. et al., 2003. Carbon balance of a tropical savanna of northern Australia. *Oecologia*, 137(3), pp.405–416.

Cohen, C.J., 2000. Early History of Remote Sensing. In *Remote Sensing*. London: Oxford University Press, pp. 3–9.

Complexity Academy, 2016. Ecosystem Dynamics. *Complexity Academy*. Available at: http://complexityacademy.io/ecosystem-dynamics/ [Accessed October 9, 2016].

Cowie, I.D., 2013. NT Flora. *Northern Territory flora online*. Available at: http://eflora.nt.gov.au/factsheet?id=21101 [Accessed March 28, 2017].

Dai, L. et al., 2015. Relation between stability and resilience determines the performance of early warning signals under different environmental drivers. *Proceedings of the National Academy of Sciences*, 112(32), pp.10056–10061.

De Keersmaecker, W. et al., 2015. A model quantifying global vegetation resistance and resilience to short-term climate anomalies and their relationship with vegetation cover. *Global Ecology and Biogeography*, 24(5), pp.539–548.

De Keersmaecker, W. et al., 2015. Species-rich semi-natural grasslands have a higher resistance but a lower resilience than intensively managed agricultural grasslands in response to climate anomalies. *Journal of Applied Ecology*, 53, pp.430–439.

Donohue, I. et al., 2016. Navigating the complexity of ecological stability. *Ecology Letters*, 19(9), pp.1172–1185.

Donohue, R.J. et al., 2009. Climate-related trends in Australian vegetation cover as inferred from satellite observations, 1981-2006. *Global Change Biology*, 15(4), pp.1025–1039.

Fensham, R.J. et al., 2002. Quantitative assessment of vegetation structural attributes from aerial photography. *International Journal of Remote Sensing*, 23(11), pp.2293–2317.

Filatov, N. et al., 2005. *White sea. Its Marine Environment and Ecosystem Dynamics Influenced by Global Change*, Chichester, UK: Praxis Publishing Ltd.

Fox, I. et al., 2001. The Vegetation of the Australian Tropical Savannas. *Environmental Protection Agency*, p.75.

Frazier, S., 2017. MODIS Web. *Moderate Resolution Imaging Spectroradiometer*. Available at: https://modis.gsfc.nasa.gov/about/specifications.php [Accessed March 7, 2017].

Gallant, A.J.E. et al., 2013. The characteristics of seasonal-scale droughts in Australia, 1911-2009. *International Journal of Climatology*, 33(7), pp.1658–1672.

Gosling, S.N., 2013. The likelihood and potential impact of future change in the large-scale climate-earth system on ecosystem services. *Environmental Science and Policy*, 27, pp.15–31.

Guerschman, J.P. et al., 2009. Estimating fractional cover of photosynthetic vegetation, non-photosynthetic vegetation and bare soil in the Australian tropical savanna region upscaling the EO-1 Hyperion and MODIS sensors. *Remote Sensing of Environment*, 113(5), pp.928–945.

Hansen, M.C. et al., 2002. Development of a MODIS tree cover validation data set for Western Province, Zambia. *Remote Sensing of Environment*, 83(1–2), pp.320–335.

Hill, M.J. et al., 2012. Dynamics of vegetation indices in tropical and subtropical savannas defined by ecoregions and Moderate Resolution Imaging Spectroradiometer (MODIS) land cover. *Geocarto International*, 27(2), pp.153–191.

Holling, C.S., 1996. Engineering Resilience versus Ecological Resilience. In *Engineering Within Ecological Constraints*. Washington, D.C.: National Academies Press, p. 213.

House, J.I. & Hall, D.O., 2001. Productivity of Tropical Savannas and Grasslands. In *Terrestrial Global Productivity*. Elsevier, pp. 363–400.

Hughes, L., 2003. Climate Change and Australia: Trends, Projection and Impacts. *Austral Ecology*, 28, pp.423–443.

Hull, P.M. et al., 2015. Rarity in mass extinctions and the future of ecosystems. *Nature*, 528(7582), pp.345–351.

Hutley, L.. & Beringer, J., 2011. Disturbance and climatic drivers of carbon dynamics of a north Australian tropical savanna. *Ecosystem Function in Savannas: Measurement and Modeling at Landscape to Global Scales.*, pp.57–75.

Hutley, L.B. et al., 2013. Impacts of an extreme cyclone event on landscape-scale savanna fire, productivity and greenhouse gas emissions. *Environmental Research Letters*, 8(4), p.45023.

IPCC, 2014. *Climate Change 2014: Synthesis Report. Contribution of Working Groups I, II and III to the Fifth Assessment Report of the Intergovernmental Panel on Climate Change*,

Jacklyn, P. et al., 2016. Savanna Explorer - All Regions - Northern Australia. *The Tropical Savannas CRC*. Available at: http://www.savanna.org.au/all/faq.html [Accessed October 24, 2016].

Jones, H.G. & Vaughan, R.A., 2010. *Remote Sensing of Vegetation. Principles, techniques and applications*, Oxford: Oxford University Press.

Kanniah, K.D. et al., 2011. Environmental controls on the spatial variability of savanna productivity in the Northern Territory, Australia. *Agricultural and Forest Meteorology*, 151(11), pp.1429–1439.

Karlson, M. et al., 2014. Tree crown mapping in managed woodlands (Parklands) of semi-arid West Africa using WorldView-2 imagery and geographic object based image analysis. *Sensors (Switzerland)*, 14(12), pp.22643–22669.

Keitt, T.H., 2008. Coherent ecological dynamics induced by large-scale disturbance. *Nature*, 454(7202), pp.331–334.

Khorram, S. et al., 2012. *Remote Sensing*, New York: International Space University.

Krishnapuram, B. et al., 2005. Sparse multinomial logistic regression: Fast algorithms and generalization bounds. *IEEE Transactions on Pattern Analysis and Machine Intelligence*, 27(6), pp.957–968.

Laurance, W.F. et al., 2011. The 10 Australian ecosystems most vulnerable to tipping points. *Biological Conservation*, 144(5), pp.1472–1480.

Lawes, M.J. et al., 2011. How do small savanna trees avoid stem mortality by fire? The roles of stem diameter, height and bark thickness. *Ecosphere*, 2(4), p.13.

Lehmann, C.E.R. et al., 2011. Deciphering the distribution of the savanna biome. *New Phytologist*, 191(1), pp.197–209.

Lehmann, C.E.R. et al., 2014. Savanna Vegetation-Fire-Climate Relationships Differ Among Continents. *Science*, 343(January), pp.548–553.

Lehmann, C.E.R., Prior, L.D. & Bowman, D.M.J.S., 2009. Decadal dynamics of tree cover in an australian tropical Savanna. *Austral Ecology*, 34(6), pp.601–612.

Lhermitte, S. et al., 2011. A comparison of time series similarity measures for classification and change detection of ecosystem dynamics. *Remote Sensing of Environment*, 115(12), pp.3129–3152.

Liu, F-J. et al., 2015. Assessment of the three factors affecting Myanmar's forest cover change using Landsat and MODIS vegetation continuous fields data. *International Journal of Digital Earth*, 8947(July 2016), pp.1–24.

Liu, Y.Y. et al., 2009. An analysis of spatiotemporal variations of soil and vegetation moisture from a 29-year satellite-derived data set over mainland Australia. *Water Resources Research*, 45(7), pp.1–12.

Ma, X. et al., 2013. Spatial patterns and temporal dynamics in savanna vegetation phenology across the north australian tropical transect. *Remote Sensing of Environment*, 139, pp.97–115.

Martz, E., 2013. When more is not better. *Quality*, 52(August), pp.24–25.

Mašková, Z. et al., 2008. Normalized difference vegetation index (NDVI) in the management of mountain meadows. *Boreal Environment Research*, 13(5), pp.417–432.

Mitchard, E.T. a & Flintrop, C.M., 2013. Woody encroachment and forest degradation in sub-Saharan Africa's woodlands and savannas 1982-2006. *Philosophical Transactions of the Royal Society B: Biological Sciences*, 368(1625), p.20120406.

MODIS Land Team, 2016. Status for: Vegetation Continuous Fields (MOD44). *Validation*. Available at: https://landval.gsfc.nasa.gov/ProductStatus.php?ProductID=MOD44 [Accessed March 26, 2017].

Mori, A.S., 2011. Ecosystem management based on natural disturbances: Hierarchical context and non-equilibrium paradigm. *Journal of Applied Ecology*, 48(2), pp.280–292.

Muir, J. et al., 2011. *Field measurement of fractional ground cover: a technical handbook supporting ground cover monitoring for Australia* the Queensland Department of Environment and Resource Management, ed., Canberra: Australian Bureau of Agricultural and Resource Economics and Sciences.

Murphy, B.P. et al., 2014. Fire regimes and woody biomass dynamics in Australian savannas. *Journal of Biogeography*, 41(1), pp.133–144.

Nicholls, N. et al., 1997. Australian rainfall variability and change. *Weather*, 52(3), pp.66–72.

O'Grady, A.P. et al., 2000. Composition, leaf area index and standing biomass of eucalypt open forests near Darwin in the Northern Territory, Australia. *Australian Journal of Botany*, 48(5), pp.629–638.

Olson, D.M. et al., 2001. Terrestrial Ecoregions of the World: A New Map of Life on Earth. *BioScience*, 51(11), p.933.

Osborne, C.P. & Beerling, D.J., 2006. Nature's green revolution: the remarkable evolutionary rise of C4 plants. *Philosophical transactions of the Royal Society of London. Series B, Biological sciences*, 361(1465), pp.173–94.

Rasmussen, M.O. et al., 2011. Tree survey and allometric models for tiger bush in northern Senegal and comparison with tree parameters derived from high resolution satellite data. *International Journal of Applied Earth Observation and Geoinformation*, 13(4), pp.517–527.

Reznicek, A., 2008. Cyperaceae. *Encyclopedia Britannica*. Available at: https://www.britannica.com/plant/Cyperaceae [Accessed March 28, 2017].

van Rooijen, N.M. et al., 2015. Plant Species Diversity Mediates Ecosystem Stability of Natural Dune Grasslands in Response to Drought. *Ecosystems*, 18(8), pp.1383–1394.

Rouse, J.W. et al., 1973. Monitoring vegetation systems in the great plains with ERTS. *Third Earth Resources Technology Satellite (ERTS) symposium*, 1, pp.309–317.

Sangha, K.K., 2006. The role of ecosystem services from tropical savannas in well-being of Aboriginal people : A scoping study. *Tropical Savannas Cooperative Research Centre*, p.78.

Schaaf, C.B. et al., 2002. First operational BRDF, albedo nadir reflectance products from MODIS. *Remote Sensing of Environment*, 83, pp.135–148.

Scheffer, M. et al., 2009. Early-warning signals for critical transitions. *Nature*, 461(September), pp.53–59.

Scheiter, S. et al., 2014. Climate change and long-term fire management impacts on Australian savannas. *New Phytologist*, 2015(205), pp.1211–1226.

Scheiter, S. & Higgins, S.I., 2009. Impacts of climate change on the vegetation of Africa: An adaptive dynamic vegetation modelling approach. *Global Change Biology*, 15(9), pp.2224–2246.

Scholes, R.J. & Archer, S.R., 1997. Tree-Grass Interactions in Savannas. *Ecology and Systematics*, 28, pp.517–544.

Simon, B., 2010. Fact Sheets | AusGrass2. *Grasses of Australia*. Available at: http://ausgrass2.myspecies.info/content/fact-sheets [Accessed March 28, 2017].

Tom, G. et al., 2008. The Need for Global Topography. , pp.1–43.

Townshend, J.R.. et al., 2011. Vegetation Continuous Fields MOD44B, 2010 Percent Tree Cover. *Collection 5, University of Maryland, College Park, Maryland*, pp.1–12.

Verbesselt, J. et al., 2010. Detecting trend and seasonal changes in satellite image time series. *Remote Sensing of Environment*, 114(1), pp.106–115.

Vicente-Serrano, S.M. et al., 2010. A Multiscalar Drought Index Sensitive to Global Warming: The Standardized Precipitation Evapotranspiration Index. *Journal of Climate*, 23(7), pp.1696–1718.

Weisberg, P.J. et al., 2007. Spatial Patterns of Pinyon–Juniper Woodland Expansion in Central Nevada. *Rangeland Ecology & Management*, 60(2), pp.115–124.

Werner, P.A. et al., 2008. Growth and survival of termite-piped Eucalyptus tetrodonta and E. miniata in northern Australia: Implications for harvest of trees for didgeridoos. *Forest Ecology and Management*, 256(3), pp.328–334.

Wissel, C., 1984. A Universal Law of the Characteristic Return Time near Thresholds. *Oecologia*, 65(1), pp.101–107.

Zhou, Q. et al., 2016. Retrieving understorey dynamics in the Australian tropical savannah from time series decomposition and linear unmixing of MODIS data. *International Journal of Remote Sensing*, 37(6), pp.1445–1475.

9 VULGARIZING SUMMARY

The Australian tropical savannas are a unique and dynamic ecosystem, thriving on the tight coexistence between the continuous grass layer that is seasonally changing and thus controlling the dynamics of this ecosystem, and the scattered woody cover layer that lies at the base of the productivity of this ecosystem. With the ongoing climate change more extremes such as heatwaves, droughts, floods, cyclones and wildfires will occur more frequently and at higher intensities. These climate extremes and anomalies reveal significant vulnerability and exposure of some ecosystems, among which the Australian tropical savannas. In order to define the future prospects of this ecosystem, understanding and quantifying the woody cover dynamics and how this changing vegetation responds to short-term climate anomalies is of utmost importance. In this perspective, this study focuses on Litchfield National Park, situated in northern Australia, and aims to (i) quantify the woody cover dynamics from 2002 to 2016 using satellite observations and (ii) define the impact of these woody cover dynamics on the ecosystem's short-term stability in space and time. Woody cover was found to slightly increase up to 2.29% of the overall mean woody cover in this time period, confirming that woody thickening is taking place in Litchfield National Park. This increase in woody cover can mainly be attributed to the variability in climate, a changing fire regime and a rising CO_2 level. The short-term stability is in this study quantified as the vegetation resilience and variance to short-term climate anomalies, highlighting how quick vegetation recovers from these anomalies or how susceptible it is to these anomalies respectively. The impact of this woody cover increase on the resilience pointed towards a faster recovering and thus more resilient ecosystem. A growth in woody cover gave on the other hand contrasting results in space and time, with an overall increase in variance at the spatial level and a decreasing variance at the temporal level, giving no closure yet on this subject. As stability may be driven by other variables besides the woody cover, impacts of both fire frequency and bare soil coverage on the stability were analysed as well. Results of fire frequency at the spatial level indicated a lower resilience and a higher variance, corresponding to a higher susceptibility of the ecosystem, but could not be confirmed at the temporal level. Increases in bare soil coverage lastly had again a positive impact on the ecosystem as it fastened the recovery speed, making it more resilient, and decreased the variance, making it less susceptible to climate anomalies. It has however to be taken into account that woody cover, fire frequency and bare soil coverage are correlated, causing biased effects of each factor separately, and thus results from this study require to be addressed with caution.